European Journal of Medicinal Chemistry 210 (2021) 112950

Contents lists available at ScienceDirect

European Journal of Medicinal Chemistry

journal homepage: http://www.elsevier.com/locate/ejmech

Research paper

Novel σ_1 antagonists designed for tumor therapy: Structure – activity relationships of aminoethyl substituted cyclohexanes

Nicole Kopp [a], Catharina Holtschulte [a], Frederik Börgel [a], Kirstin Lehmkuhl [a], Kristina Friedland [b], Gianluca Civenni [c], Erik Laurini [d], Carlo V. Catapano [c], Sabrina Pricl [d, e], Hans-Ulrich Humpf [f], Dirk Schepmann [a], Bernhard Wünsch [a, g, *]

[a] Institut für Pharmazeutische und Medizinische Chemie, Westfälische Wilhelms-Universität Münster, Corrensstraße 48, D-48149 Münster, Germany
[b] Pharmacology and Toxicology, Pharmacy and Biochemistry, Johannes Gutenberg University, Staudingerweg 5, 55128 Mainz, Germany
[c] Institute of Oncology Research, Universita Della Svizzera Italiana (USI), Via Vincenzo Vela 6, CH-6500 Bellinzona, Switzerland
[d] Molecular Biology and Nanotechnology Laboratory (MolBNL@UniTS), DEA, University of Trieste, 34127, Trieste, Italy
[e] Department of General Biophysics, Faculty of Biology and Environmental Protection, University of Lodz, Lodz, Poland
[f] Institut für Lebensmittelchemie, Westfälische Wilhelms-Universität Münster, Corrensstraße 45, D-48149 Münster, Germany
[g] Cells-in-Motion Cluster of Excellence (EXC 1003 – CiM), Westfälische Wilhelms-Universität Münster, Germany

ARTICLE INFO

Article history:
Received 23 July 2020
Received in revised form
19 September 2020
Accepted 14 October 2020
Available online 22 October 2020

Keywords:
σ receptors
Aminoethylcyclohexanes
Stereochemistry
Chiral HPLC
CD spectroscopy
σ_1 receptor affinity
Selectivity
Structure affinity relationships
Molecular interactions
Molecular dynamics simulations
Calculated free energy of binding
per-residue binding free energy
Voltage gated Ca^{2+} channel
Ca^{2+} influx assay
Antagonistic activity
Inhibition of human prostate tumor cell growth
DU145 tumor cells
Lipophilicity
Biotransformation

ABSTRACT

Depending on the substitution pattern and stereochemistry, 1,3-dioxanes **1** with an aminoethyl moiety in 4-position represent potent σ_1 receptor antagonists. In order to increase the stability, a cyclohexane ring first replaced the acetalic 1, 3-dioxane ring of **1**. A large set of aminoethyl substituted cyclohexane derivatives was prepared in a six-step synthesis. All enantiomers and diastereomers were separated by chiral HPLC at the stage of the primary alcohol **7**, and their absolute configuration was determined by CD spectroscopy. Neither the relative nor the absolute configuration had a large impact on the σ_1 affinity. The highest σ_1 affinity was found for cis-configured benzylamines (1R,3S)-**11** ($K_i = 0.61$ nM) and (1S,3R)-**11** ($K_i = 1.3$ nM). Molecular dynamics simulations showed that binding of (1R,3S)-**11** at the σ_1 receptor is stabilized by the typical polar interaction of the protonated amino moiety with the carboxy group of E172 which is optimally oriented by an H-bond interaction with Y103. The lipophilic interaction of I124 with the N-substituent also contributes to the high σ_1 affinity of the benzylamines. The antagonistic activity was determined in a Ca^{2+} influx assay in retinal ganglion cells. The enantiomeric cis-configured benzylamines (1R,3S)-**11** and (1S,3R)-**11** were able to inhibit the growth of DU145 cells, a highly aggressive human prostate tumor cell line. Moreover, cis-**11** could also inhibit the growth of further human tumor cells expressing σ_1 receptors. The experimentally determined $logD_{7.4}$ value of 3.13 for (1R,3S)-**11** is in a promising range regarding membrane penetration. After incubation with mouse liver microsomes and NADPH for 90 min, 43% of the parent (1R,3S)-**11** remained unchanged, indicating intermediate metabolic stability. Altogether, nine metabolites including one glutathione adduct were detected by means of LC-MS analysis.

1. Introduction

Originally, the σ receptor has been classified as an opioid receptor subtype [1]. Further studies showed that the effects of the prototypical σ receptor agonist (+)-SKF-10,047 could not be antagonized by the opioid receptor antagonist naltrexone;

* Corresponding author. Institut für Pharmazeutische und Medizinische Chemie, Westfälische Wilhelms-Universität Münster, Corrensstraße 48, D-48149 Münster, Germany.
E-mail address: wuensch@uni-muenster.de (B. Wünsch).

https://doi.org/10.1016/j.ejmech.2020.112950
0223-5234/

therefore, the σ receptor was no longer considered as a member of the opioid receptor family [2]. In the early 1990s, two σ receptor subtypes were distinguished based on their different binding profile of benzomorphans and they were termed σ_1 and σ_2 receptor, respectively [3,4]. The σ_1 receptor subtype was already cloned in 1996 from different tissues (brain, liver, choriocarcinoma cell line) of different species (rat, mouse, guinea pig, human) [5–9]. The σ_2 receptor, however, was not characterized until 2017, when it was isolated from calf liver tissue and identified as the endoplasmic reticulum (ER)-resident transmembrane protein 97 (TMEM97) [10]. In contrast to the σ_2 receptor, which is a protein of 176 amino acids (Mw ~20.8 kDa) whose three-dimensional structure has not been solved yet, the human σ_1 receptor (223 amino acids, Mw ~25.3 kDa) was crystallized recently [11,12].

The σ_1 receptor is widely expressed in the central nervous system (CNS) and various peripheral organs including liver, heart, kidney and the eye [13–16]. It is involved in central nervous system (CNS) pathologies such as schizophrenia, depression, Alzheimer's disease and drug/alcohol dependence [17–22]. Therefore, σ_1 receptor ligands can find application as potential therapeutics for the treatment of various CNS disorders including neuropathic pain [23,24] and depression.

Furthermore, an increased expression of σ_1 receptors in cancer cell lines and human tumors has been reported [25,26]. The increased expression of σ_1 receptor in human cancer cell lines and human tumors raises the possibility that σ_1 receptor modulators might be therapeutically beneficial also for treating cancer in addition to neurological disorders [25,26]. Analysis of large public databases with gene and protein expression data in human cell lines and tumor samples shows expression of σ_1 receptors in many hematological and solid tumor types, including prostate, breast, bladder, colon, and lung cancer [26]. Indeed, the widespread expression of σ_1 receptors across tumor types of different histology and the heterogeneity of its expression in tumors and cell lines within the same subtypes suggest that the σ_1 receptor is an important modulator of key biological processes in cancer cells acting in a context-dependent manner [26,27]. Its functions in cancer cells might be particularly relevant in the context of stress response, metabolic plasticity and activation of adaptive and survival mechanisms [28–32]. Importantly, upon treatment with various σ_1 receptor modulators reduction of cell proliferation and survival of tumor cells was observed [32–35]. However, the underlying mechanisms and the specificity of the observed effects have not been fully understood [26,27].

In this project, novel highly selective σ_1 receptor ligands will be developed with a strong potential to target cancer cells. Recently, we have reported on various 1,3-dioxanes **1** with various aminoethyl substituents in 4-position (Fig. 1). Depending on the absolute configuration, the substitution pattern at the acetalic 2-position and the amino group, compounds **1** displayed high affinity towards either the σ_1 receptor or the phencyclidine (PCP) binding site of the NMDA receptor. As an example, the (2S,4R)-configured benzylamine **1a** derived from benzaldehyde showed very high affinity towards the σ_1 receptor (K_i = 6.0 nM), but only negligible affinity towards the PCP binding site (K_i > 10 μM). On the other hand, the (2R,4R)-configured primary amine **1b** derived from propiophenone exhibited high affinity towards the PCP binding site (K_i = 13 nM), but very low affinity towards σ_1 receptors (K_i > 10 μM) [36], The racemic benzylamine **1a** ($K_i(\sigma_1)$ = 19 nM [37]. showed very high antiallodynic activity in vivo in the mouse capsaicin assay [38]. This analgesic activity thus confirmed the σ_1 antagonistic activity of racemic benzylamine 1a.

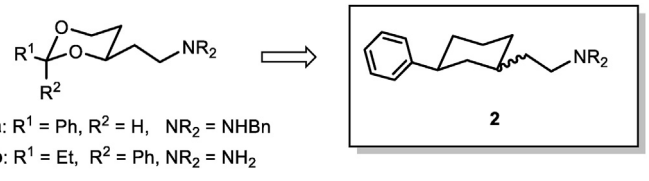

Fig. 1. Lead compounds **1** for the development of novel potent σ_1 receptor antagonists **2** based on the cyclohexane ring.

Although the in vitro and even the in vivo (intraperitoneal application) pharmacological profile of the 1,3-dioxane **1a** appeared to be promising, its acetalic nature limits its practical use. In particular, fast hydrolysis of the acetal in the stomach after peroral application is expected. Therefore, the acetalic substructure of **1a** should be replaced by a more stable structural element. In a first attempt toward this direction, we considered the replacement of the O-atoms in the 1,3-dioxane by two CH_2-moieties, which resulted in cyclohexane derivatives **2** (Fig. 1). Herein, we now report the synthesis and pharmacological evaluation of cyclohexanes **2** with various amino moieties with a particular emphasis on the stereochemistry of this novel class of σ ligands.

2. Chemistry

2.1. Synthesis

The synthesis of the designed cyclohexane derivatives **2** started with a Rh-catalyzed conjugate addition of phenylboronic acid at cyclohexenone (**3**) [39]. (Scheme 1) Using Rh $(cod)_2BF_4$ as catalyst in hot dioxane/KOH provided the addition product **4** in 86% yield. Wittig reaction of the ketone **4** with the stabilized P-Ylid $Ph_3P{=}CHCO_2CH_3$ led to the α,β-unsaturated ester **5** as 53:47 mixture of (E)/(Z)-diastereomers. Hydrogenation of the α,β-unsaturated ester **5** using the catalyst Pd/C afforded cis- and trans-configured saturated esters **6** in the ratio 75 : 25.

The primary alcohol **7** was obtained by $LiAlH_4$ reduction of ester **6**. Two different routes were pursued to prepare the amines **10**–**15** from the primary alcohol **7**. Upon treatment with $Zn(N_3)_2$ py_2, PPh_3 and DIAD [40], the alcohol **7** was converted into the azide **8**, which was reduced with H_2, Pd/C to give the primary amine **10**. Alternatively, the primary alcohol **7** was transformed into the mesylate **9**, which could be substituted by various primary and secondary amines to yield the amines **11**–**15** (Scheme 1).

During the hydrogenation of the α,β-unsaturated ester **5** a second center of chirality was established. The ester was obtained as 75 : 25 mixture of diastereomers cis-**6**: trans-**6**. The same ratio of diastereomers was found for all products **7**–**15** derived from ester **6**. In the ^1H NMR spectra of the compounds **6**–**15** a quartet-like signal with three rather large coupling constants of 12.1–12.3 Hz at 1.0–1.2 ppm was found for the axially oriented proton in 2-position of the major diastereomer. Such a signal structure caused by a geminal coupling and two 1,2-trans-diaxial couplings is only possible if both substituents in 1- and 3-position adopt an equatorial orientation, i.e. cis-configuration.

2.2. Stereochemistry

The amines were obtained as 75 : 25 mixture of diastereomers, which could not be separated by flash chromatography. Therefore, the diastereomers were separated by preparative HPLC on a RP18 Phenomenex Gemini 5 μm column on a preparative scale. The diastereomeric benzylamines **11** and phenylpiperazines **15** were separated with an eluent mixture of CH_3CN, H_2O and NEt_3 (0.1%), whereas the pyrrolidine diastereomers cis-**14** and trans-**14** were separated using a CH_3OH, H_2O and NEt_3 (0.1%) mobile phase. (HPLC methods A1-A3).

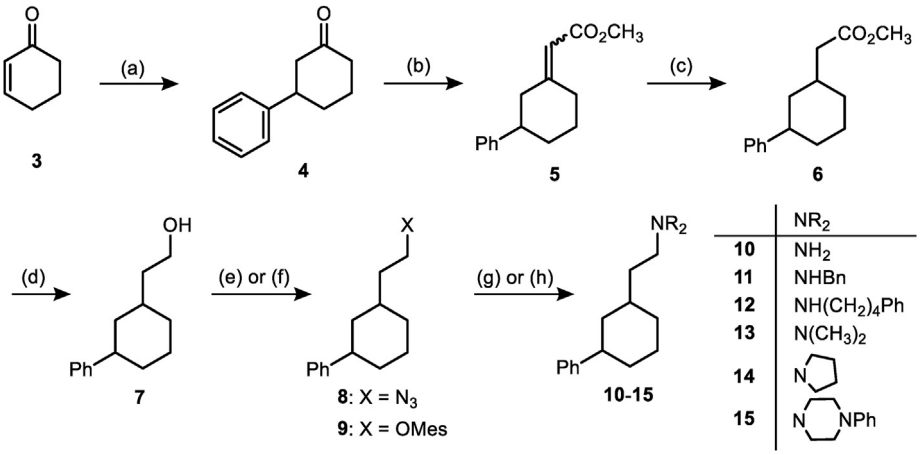

Scheme 1. Synthesis of amines 10–15. Reagents and reaction conditions: (a) $PhB(OH)_2$, Rh $(cod)_2BF_4$, dioxane/1.5 M KOH (3:1), 90 °C, 4.5 h, 86%. (b) $Ph_3P{=}CHCO_2CH_3$, toluene, 110 °C, 17 h, 89%. (c) H_2 (balloon), Pd/C, CH_3OH, rt, 15 min, 83%. (d) $LiAlH_4$, THF, 0 °C, 30 min, then rt, 2 h, 91%. (e) $Zn(N_3)_2$ py_2, PPh_3, DIAD, toluene, rt, 6 h, 73% (8) [40]. (f) CH_3SO_2Cl, CH_2Cl_2, NEt_3, rt, 22 h, 85% (9). (g) 8: H_2 (balloon), Pd/C, CH_3OH, rt, 2 h, 32% (10). (h) 9: R_2NH, CH_3CN, 82 °C, 15–27 h, or microwave (for 13), 72–89% (11–15). The ratio of diastereomers cis: trans = 75 : 25.

Since the diastereomeric racemic benzylamines cis-**11** (K_i = 1,8 ± 0.19 nM) and trans-**11** (K_i = 2.4 ± 0.17 nM) showed high σ_1 affinity, the enantiomers of cis-**11** and trans-**11** should be separated and investigated pharmacologically. Separation of the benzylamine enantiomers **11** turned out to be difficult. Therefore, the stereoisomeric alcohols **7** were separated by preparative chiral HPLC using a Daicel Chiralpak IB column (250 mm, 20 mm, HPLC method B) as stationary phase. The chromatogram displayed in Fig. 2 shows the separation of all four stereoisomers (1R,3R)-**7**, (1R,3S)-**7**, (1S,3S)-**7**, and (1S,3R)-**7**. It should be noted that each pair of enantiomers ((1R,3R)-**7**/(1S,3S)-**7** and (1R,3S)-**7**/(1S,3**R**)-7, respectively) is well separated, whereas the pairs of diastereomers ((1R, R)-**7**/(1R,3S)-**7** and (1S,3S)-**7**/(1S,3R)-**7**, respectively) have very similar retention times. Therefore, it can be concluded that separation of these molecules at the diastereomer level appears to be difficult, while the same process becomes less problematic when dealing with the corresponding enantiomers.

After successful separation of the four stereoisomeric alcohols **7**, the stereochemical purity was assessed by chiral analytical HPLC. In each sample the amount of the desired stereoisomer was higher than 98.57% indicating high stereochemical purity of the alcohols **7** (see Table S2 (Supporting Information)).

The stereoisomeric alcohols **7** were next transformed into the stereoisomeric benzylamines **11** as described for the mixture of diastereomers. At first, the alcohols **7** were converted into the mesylates **9**, which were substituted with benzylamine to afford the four stereoisomerically pure benzylamines (1R,3S)-**11**, (1S,3R)-**11**, (1R,3R)-**11**, and (1S,3S)-**11** (Scheme 2).

In order to produce large amounts of enantiomerically pure benzylamines **11**, the stereoisomers were separated by an alternative method. At first, chiral HPLC was used to separate the enantiomers of the alcohol **7** without separating the diastereomers; this separation could be performed on large amounts due to the big difference in retention times (see Fig. 2). Thus, after performing the chiral HPLC, enantiomerically pure mixtures of diastereomers (1R,3S)-**7**+(1R,3R)-**7** and (1S,3R)-**7**+(1S,3S)-**7** were obtained (HPLC method C). The mixtures of diastereomeric alcohols (1R, 3S)-**7**+(1R,3R)-**7** and (1S,3R)-**7**+(1S,3S)-**7** were then converted into benzylamines (1R,3S)-**11**+(1R,3R)-**11** and (1S,3S)-**11**/(1S,3S)-**11**. Finally, the pairs of diastereomeric benzylamines could be easily separated by preparative RP-HPLC to achieve the diastereomerically and enantiomerically pure benzylamines (1R,3S)-**11**, (1R,3R)-**11**, (1S,3R)-**11**, and (1S,3S)-**11** (HPLC method D).

Since primary amines are of interest as NMDA receptor antagonists (compare primary amine **1b** in Fig. 1), the stereoisomerically pure benzylamines **11** should be converted into primary amines **10** upon hydrogenolytic removal of the benzyl moiety. In the first reactions methanolic solutions of benzylamines (1R 3S)-**11** and (1S,3R)-**11** were treated with H_2 in the presence of Pd/C as catalyst. However, instead of the primary amines (1R,3S)-**10** and (1S,3R)-**10**, the dimethylamines (1R,3S)-**13** and (1S,3R)-**13**, were formed. The unexpected methylation was explained by a Pd-catalyzed dehydrogenation of CH_3OH to afford formaldehyde, which in turn underwent reductive alkylation of primary and secondary amines [41]. This methylation could be avoided by using the solvent THF instead of CH_3OH. However, in THF higher H_2 pressure and longer reaction times were required to reach complete debenzylation of benzylamines 11. Thus, the stereoisomeric primary amines (1R,3S)-**10**, (1S,3R)-**10**, (1R,3R)-**10**, and (1S,3S)-**10** were obtained in 30–48% yields.

In order to analyze the absolute configuration of the stereoisomeric benzylamines, circular dichroism (CD) spectra of (1R,3S)-**11**, (1S,3R)-**11**, (1R,3R)-**11**, and (1S,3S)-**11** were recorded. Figs. 3 and 4 show the CD spectra of the enantiomeric cis-configured benzylamines (1R,3S)-**11** and (1S,3R)-**11** and of the enantiomeric trans-

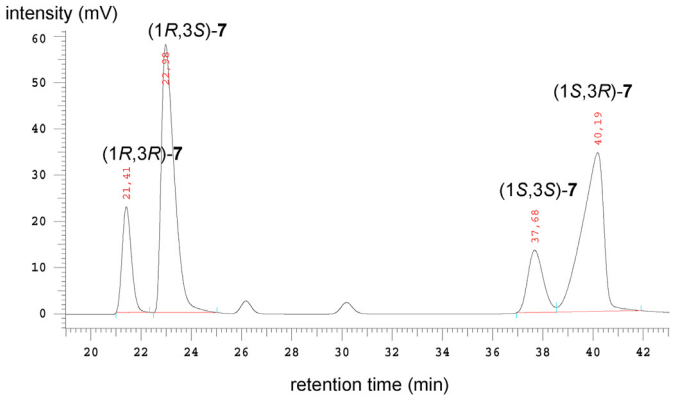

Fig. 2. HPLC chromatogram of the separation of stereoisomeric alcohols **7**. HPLC method B: Daicel Chiralpak IB 5 μm, 250 mm, 20 mm, isohexane: isopropanol = 98 : 2, 19 mL/min, detection at λ = 210 nm.

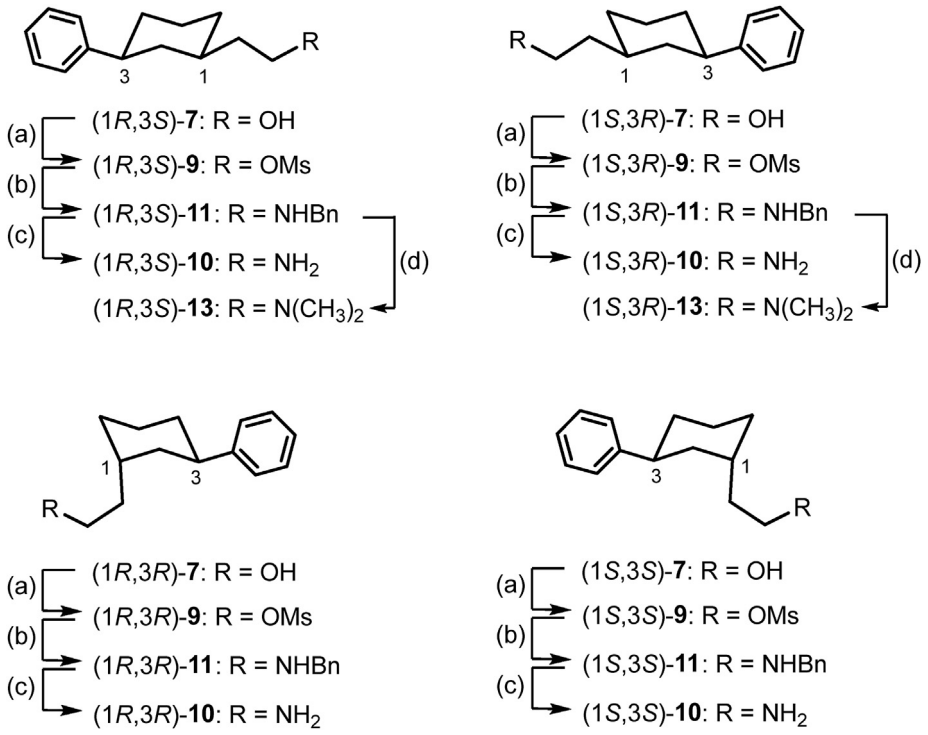

Scheme 2. Synthesis of enantiomerically pure primary amines **10**, benzylamines **11** and dimethylamines **13**: Reagents and reaction conditions: (a) f) CH_3SO_2Cl, CH_2Cl_2, NEt_3, rt, 87–92%. (b) $BnNH_2$, CH_3CN, 82 °C, 15–23 h, 83–89%. (c) H_2 (5 bar), Pd/C, THF, 25–27 h, 40–81%. (d) H_2 (balloon), Pd/C, CH_3OH, HOAc (2 drops), 6–20 h, 30–48%.

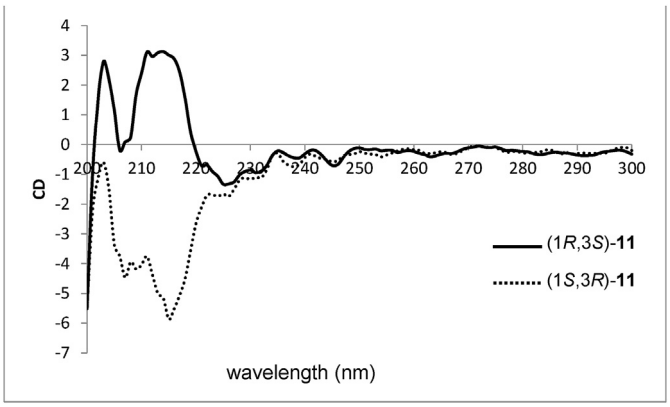

Fig. 3. CD spectra (CH_3CN) of enantiomeric cis-configured benzylamines (1R,3S)-**11** and (1S,3R)-**11**.

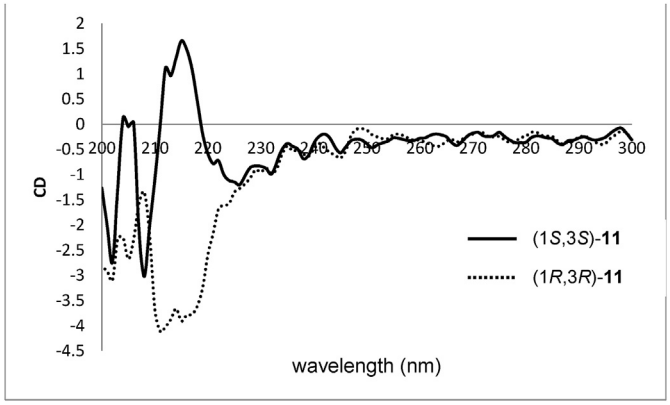

Fig. 4. CD spectra (CH_3CN) of enantiomeric trans-configured benzylamines (1S,3S)-**11** and (1R,3R)-**11**.

configured benzylamines (1R,3R)-**11** and (1S,3S)-**11**, respectively.

From these images it can be clearly seen that the stereoisomers with a (3S)-configuration of the center of chirality adjacent to the phenyl ring show a positive Cotton effect at approx. 210 nm, whereas the benzylamines with the alternative (3R)-configuration exhibit mirror-image spectra characterized by a negative Cotton effect at the same wavelength.

To determine the absolute configuration of the stereoisomeric benzylamines CD spectra of the model compounds (1R,3S)- and (1S, S)-1-methyl-3-phenylcyclohexane (1R,3S)-**16** and (1S,3S)-**16**) were predicted [42–44]. (Fig. 5) In order to reduce the computational time required for such calculations, the rather flexible benzylaminoethyl side chain of **11** was replaced by the small methyl moiety. Calculated CD spectra [45] of both (3S)-configured cyclohexanes **16** show a positive Cotton effect at approx. 210 nm. Therefore, (3S)-configuration was assigned to the both benzylamines (1R,3S)-**11** and (1S,3S)-**11**, which also experimentally exhibited a positive Cotton effect at the same wavelength (Fig. 5).

3. Receptor affinity

The affinity towards σ_1 and σ_2 receptors was determined in competitive receptor binding studies with radioligands, i.e., [^{3}H](+)-pentazocine for σ_1 assay and [^{3}H]di-o-tolylguanidine for σ_2 assay, respectively. Membrane preparations from guinea pig brain (σ_1 assay) and rat liver (σ_2 assay) served as receptor material. Radioactivity emitted by each receptor/radioligand complex was recorded after incubation with different concentrations of the test compounds [46–48]. Table 1 summarizes the σ_1 and σ_2 receptor affinities of the prepared amines 10–15 thus obtained.

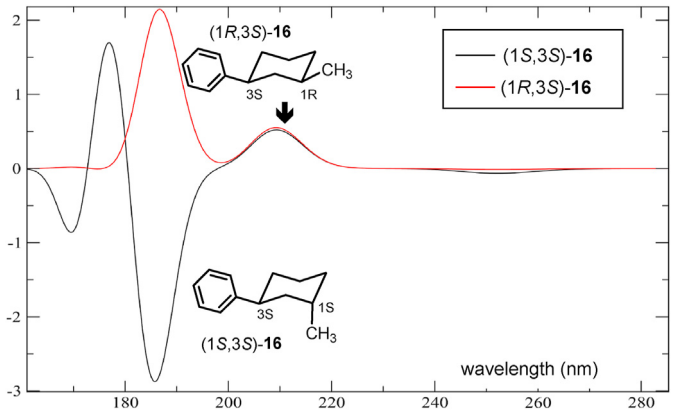

Fig. 5. Calculated CD spectra for the model compounds cis-(1R,3S)-**16** and trans-(1S,3S)-**16**.

The benzylamines **11** reveal the highest σ_1 affinity with K_i values in the low nanomolar to subnanomolar range. Extension of the distance between the terminal phenyl moiety and the basic amino group by four CH_2-moieties as in **12** provided almost the same σ_1 affinity. Compared with the benzylamines **11**, the σ_1 affinity of the tertiary dimethylamines **13** is reduced 10- to 15-fold. Whereas the large 4-phenylpiperazine derivatives **15** display almost the same σ_1 affinity as the dimethylamines **13**, the σ_1 affinity of the pyrrolidines **14** is slightly increased. The lowest σ_1 affinity within this novel compound class was found for the primary amines **10**.

In general, the relative configuration does not have a large impact on the σ_1 affinity. In all examples, cis- and trans-configured diastereomers show almost the same σ_1 affinity. Moreover, the absolute configuration also does not influence the σ_1 affinity to a large extent. The K_i values of the stereoisomeric benzylamines **11** range from 0.61 nM ((1R,3S)-**11**) to 1.8 nM ((1R,3R)-**11**). The eudismic ratio of both pairs of enantiomers is 2.2 and 1.3, respectively. A similar observation can be made for the tertiary dimethylamines (1R,3S)-**13** and (1S,3R)-**13**, exhibiting almost the same σ_1 affinity and a low eudismic ratio of 1.3. The highest eudismic ratio of 14 was found for the trans-configured primary amines (1S,3S)-**10** and (1R,3R)-**10**. However, the σ_1 affinity of the primary amines **10** is rather low, and the most potent stereoisomer (1R,3R)-**10** reveals a K_i value of 43 nM, which is more than 10-fold higher than the K_i values of benzylamines **11**, phenylbutylamine **12** and pyrrolidines **14**.

All compounds show excellent selectivity for the σ_1 receptor over the σ_2 subtype. In particular, the most potent compounds of this class of ligands, the stereoisomeric benzylamines **11**, exhibit a σ_1/σ_2 selectivity of 35- to 50-fold.

In addition to the σ_1 and σ_2 affinity, the affinity towards the PCP binding site of the NMDA receptor [36,49] was recorded. However, the compounds were not able to replace the radioligand [^{3}H](+)-MK-801 from its binding site up to a concentration of 1 μM. This result was surprising as the primary amine **1b** possesses high PCP affinity. It was concluded that the missing ethyl moiety in 3-position of primary amines **10** is responsible for their negligible PCP affinity. In **1b**, this ethyl moiety changes the orientation of the phenyl moiety at the six-membered core heterocycle, which might be the reason for the high PCP affinity of **1b** compared with primary amines **10**.

4. Molecular interactions between the novel ligands and the σ_1 receptor

Since (1R,3S)-**11** ($K_i\sigma_1 = 0.61$ nM) turned out to have the highest σ_1 affinity of this new class of ligands, molecular dynamics (MD) simulations were performed on the corresponding σ_1 receptor/(1R 3S)-**11** complex in order to gain more details on the binding mechanism of this compound to its biological target. The membrane bound 3D structure of the σ_1 receptor protein obtained by X-ray crystal structure analysis (pdb code 5HK1) was used as starting point for these calculations [11]. Thus, an optimal binding site for (1R,3S)-**11** was initially identified on σ_1 receptor (Fig. 6A and B) following a consolidated protocol [50,51]. Next, the corresponding ligand/protein free energy of binding (ΔG_{bind}) - along with the

Table 1
Affinity of prepared amines **10**–**15** towards σ_1 and σ_2 receptors as well as towards the PCP binding site of the NMDA receptor.

compd.	-NR_2	$K_i \pm$ SEM [nM] (n = 3)				
		σ_1	Eudismic ratio	σ_2[a)]	Eudismic ratio	PCP[a)]
(1R,3S)-**10**	NH_2	167 ± 68	1.2	38%	–	11%
(1S,3R)-**10**		138 ± 44		24%	–	14%
(1S,3S)-**10**		603 ± 184	14	60%	–	31%
(1R,3R)-**10**		43 ± 8,1		43%	–	15%
cis-**11**	NHBn	1.8 ± 0.19		130[b)]		11%
trans-**11**		2.4 ± 0.17		268[b)]		31%
(1R,3S)-**11**	NHBn	0.61 ± 0.12	2.2	49 ± 31	1.0	
(1S,3R)-**11**		1.3 ± 0.18		47 ± 10		
(1S,3S)-**11**		1.4 ± 0.20	1.3	46 ± 11	1.2	
(1R,3R)-**11**		1.8 ± 0.13		57 ± 7		
12 cis:trans = 75:25	$NH(CH_2)_4Ph$	3.0 ± 0.68		93 ± 9.7		11%
13 cis:trans = 75:25	$N(CH_3)_2$	4.2 ± 0.55		115[b)]		25%
(1R,3S)-**13**	$N(CH_3)_2$	14 ± 1,6	1.3	76 ± 15	2.1	
(1S,3R)-**13**		10 ± 4,8		156 ± 24		
cis-**14**		3.6 ± 1.2		61 ± 9.6		36%
trans-**14**		2.0 ± 0.98		33 ± 6.0		28%
cis-**15**	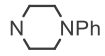	16 ± 6.8		118 ± 23		0%
trans-**15**		13 ± 3.8		144 ± 33		0%
(+)-pentazocine		5.7 ± 2.2		–		
haloperidol		6.3 ± 1.6		78 ± 2.3		
di-o-tolylguanidine		89 ± 29		58 ± 18		

[a)] Values in % describe the inhibition of radioligand binding at a test compound concentration of 1 μM.
[b)] Due to low affinity, these values were determined only once.

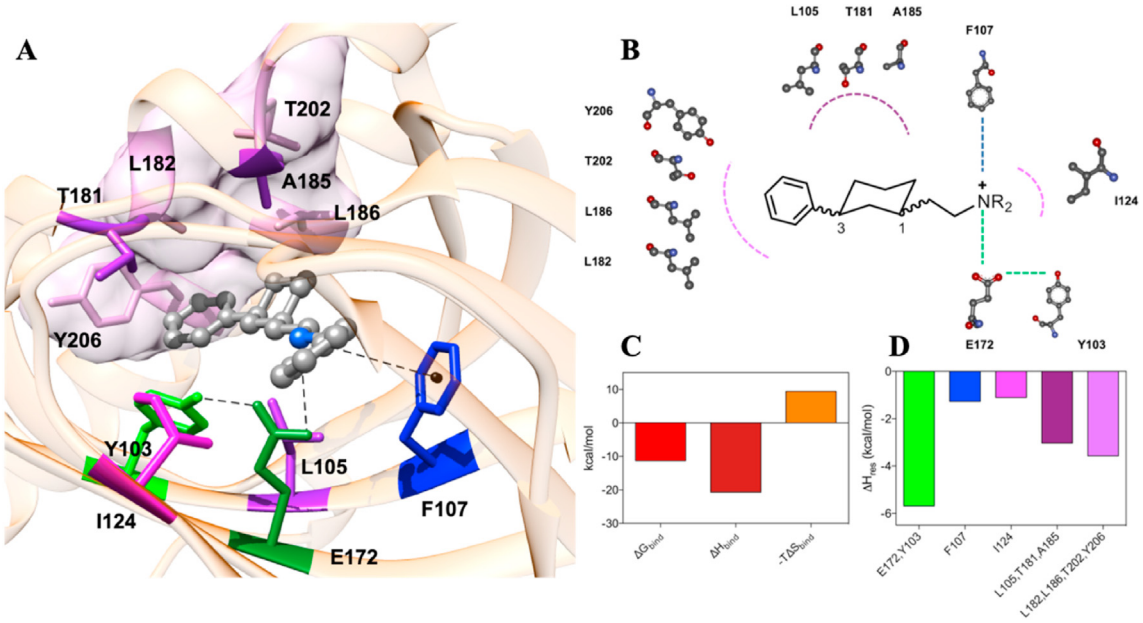

Fig. 6. (A) Details of compound (1R,3S)-**11** in the binding pocket of σ_1 receptor. (1R,3S)-**11** is shown as atom-colored sticks-and-balls (C, grey, N, blue, O, red) while the side chains of protein residues mainly interacting with (1R,3S)-**11** are depicted as colored sticks and labeled. Hydrogen atoms, water molecules, ions, and counterions are omitted for clarity. (B) 2D schematic representation of the general stabilizing interactions between the new aminoethyl substituted cyclohexanes and σ_1 receptor (C) Calculated free energy of binding (ΔG_{bind}, red), and enthalpic (ΔH_{bind}, brown-red) and entropic ($-T\Delta S_{bind}$, orange) components for: (1R,3S)-**11** complexed with the σ_1 receptor. (D) Per-residue binding free energy decomposition of the main involved amino acids of the complex between (1R,3S)-**11** and σ_1 receptor. (For interpretation of the references to color in this figure legend, the reader is referred to the Web version of this article.)

enthalpic and entropic components (ΔH_{bind} and $-T\Delta S_{bind}$, respectively) - were calculated via the MM/PBSA (Molecular Mechanics/Poisson- Boltzmann Surface Area) approach [52], yielding values in agreement with the experimental affinity (Fig. 6C and Table S3 (Supporting Information), $\Delta G_{bind} = -11.31$ kcal/mol; $\Delta H_{bind} = -20.69$ kcal/mol; $-T\Delta S_{bind} = 9.38$ kcal/mol). Finally, through a per-residue binding free energy deconvolution (PRBFED) of the enthalpic terms (ΔH_{res}), the binding mechanisms of (1R,3S)-**11** to its target protein could be defined precisely as described below. (Fig. 6D and Table S4 (Supporting Information))

Fig. 6A and B shows in detail the qualitative pattern of the interactions between (1R,3S)-**11** and the σ_1 receptor. Three receptor hydrophobic regions contribute to host the lipophilic moieties of (1R,3S)-**11**: the phenyl group in position 3 of the cyclohexane ring is encased in a receptor cavity lined by the side chains of residues L182, L186, T202 and Y206 of the membrane-proximal α-helix ($\Sigma\Delta H_{res} = -3.57$ kcal/mol); the cyclohexane ring is suitably located within a hydrophobic region made up by residues L105, T181, and A185 ($\Sigma\Delta H_{res} = -3.03$ kcal/mol); and the N-benzyl moiety performs hydrophobic interactions with I124 ($\Delta H_{res} = -1.11$ kcal/mol). Furthermore, the basic amino moiety of (1R,3S)-**11** is engaged in the σ_1-typical polar interaction with the carboxylic group of E172, oriented in an optimal position by virtue of a hydrogen bond with Y103 ($\Sigma\Delta H_{res} = -5.69$ kcal/mol). Finally, the protonated amino moiety stabilizes the binding through a π-cation interaction with the aromatic side chain of F107 ($\Delta H_{res} = -1.27$ kcal/mol).

In order to provide a quantitative SAR analysis, the same computational approach was extended to all other molecules of this new series. Accordingly, quantification of the main contributions of the single protein residues involved in ligand binding allowed to rationalize and compare the specific interactions of each tested compound with each amino acid residue in the binding cavity of the σ_1 receptor protein. (Figs. 6B and 7 and S1-3, Table S3 and S4 (Supporting Information)).

The MM/PBSA estimated values of ΔG_{bind} confirmed that all cyclohexane-based amines (with the exception of the primary amines **10**) are provided with high affinity toward the σ_1 receptor with favorable free energy values lower than −10 kcal/mol. The computational analysis substantiated that stereochemistry has only a small impact on the σ_1 binding affinity of these compounds. Indeed, all four stereoisomeric benzylamines **11** bind at the σ_1 receptor by following the same pattern of interactions as detailed above for the lead compound (1R,3S)-**11** (Fig. 7A–C, Figure S1). Finally, the free energy decomposition analysis confirmed the very small preference of the σ_1 receptor for the cis-configured benzylamines (1R,3S)-**11** and (1S,3R)-**11**. A similar preference for cis-configured derivatives was observed in a previous work on spirocyclic benzopyrans[51].

Replacement of the benzylamino moiety of **11** by smaller substituents such as the dimethylamino group in **13** or the pyrrolidine ring in **14** led to a slight decrease of the corresponding σ_1 binding capacity, quantified by a loss of about 1 kcal/mol in their ΔG_{bind} values (Fig. 7D–F, Figure S2). According to the interaction spectra shown in Fig. 7F, the reduced free energy of binding of the dimethylamine (1R,3S)-**13** and the pyrrolidine (1R,3S)-**14** can be attributed to a reduced hydrophobic interaction of I124 with the smaller alkyl groups at the N-atom. Even more dramatic is the decrease in σ_1 affinity for the primary amines 10. Although primary amine (1R,3S)-**10** exhibited the least entropic penalty of the entire series, it paid more than 2 kcal/mol in σ_1 binding efficiency, due to complete missing of interactions with I124 and the suboptimal polar and π-cation interactions with E172 and F107, respectively. (Table S4).

A larger spacer between the basic amino moiety and the terminal phenyl ring as in the phenylbutylamine **12** and the phenylpiperazine **15** is well tolerated in the σ_1 binding cavity only if the spacer is a flexible alkyl chain (e.g. (1R,3S)-**12**, Fig. 7G–I, Figure S3). In (1R,3S)-**12** the four CH_2 moieties allow an appropriate orientation of the terminal phenyl moiety to form very similar interaction spectra compared to (1R,3S)-**11**. (Table S4 (Supporting

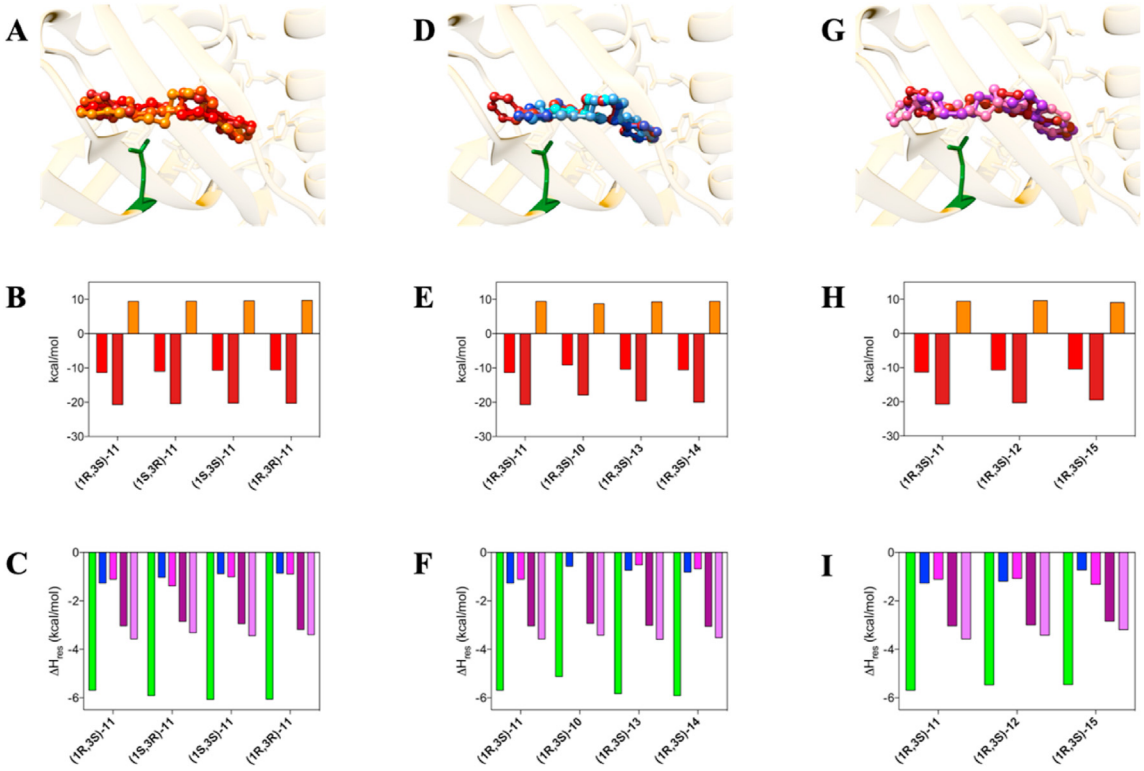

Fig. 7. Overlay of σ_1 binding modes of lead compound (1R,3S)-**11** (firebrick) with (A) (1S,3R)-**11** (red), (1S,3S)-**11** (orange red) and (1R,3R)-**11** (orange), (D) (1R,3S)-**10** (cyan), (1R 3S)-**13** (cornflower blue) and (1R,3S)-**14** (medium blue) and (G) (1R,3S)-**12** (purple) and (1R,3S)-**15** (hot pink).
Comparison of σ_1 receptor − ligand calculated free energy of binding (ΔG_{bind}, red), enthalpic (ΔH_{bind}, brown-red) and entropic ($-T\Delta S_{bind}$, orange) components of lead compound (1R,3S)-**11** with (B) (1S,3R)-**11**, (1S,3S)-**11** and (1R,3R)-**11** (E) (1R,3S)-**10**, (1R,3S)-**13** and (1R,3S)-**14** and (H) (1R,3S)-**12** and (1R,3S)-**15**.
Comparison of σ_1 receptor − ligand PRBFED analysis of lead compound (1R,3S)-**11** with (C) (1S,3R)-**11**, (1S,3S)-**11** and (1R,3R)-**11** (F) (1R,3S)-**10**, (1R,3S)-**13** and (1R,3S)-**14** and (I) (1R,3S)-**12** and (1R,3S)-**15**. The color code indicating the contribution of the respective structural elements to the free binding enthalpy is the same as given in Fig. 6C.(For interpretation of the references to color in this figure legend, the reader is referred to the Web version of this article.)

Information)). On the other hand, the more rigid piperazine spacer inhibits adopting this favorable phenyl ring orientation in (1R,3S)-**15**. Consequently, the lower σ_1 affinity of the phenylpiperazine (1R,3S)-**15** is due to a globally unfavorable binding pose in the σ_1 receptor cavity, which, in turn, reflects in substantial decreased contributions of each amino acid residue to the specific interaction with the ligand. (Fig. 7G–I).

5. Antagonistic activity: interaction with voltage-gated Ca^{2+} channels in retinal ganglion cells

The influence of the most promising σ_1 ligands cis-**11** ($K_i = 1.8$ nM), trans-**11** ($K_i = 2.4$ nM) and trans-**14** ($K_i = 2.0$ nM) on voltage dependent intracellular Ca^{2+} levels in retinal ganglion cells was investigated in a functional assay [53]. The principle of the assay is as follows: at first, the retinal ganglion cells were incubated with the Ca^{2+} sensitive fluorescent dye fura-2-AM and one of the test compounds cis-**11**, trans-**11** or trans-**14** at a concentration of 10 nM. Then, the influx of Ca^{2+} ions was induced upon treatment of the cells with KCl and the intracellular fluorescence was recorded and correlated with the intracellular Ca^{2+} concentration.

While the σ_1 agonist opipramol was able to reduce the KCl induced influx of Ca^{2+} ions into the retinal ganglion cells significantly, the aminoethyl substituted cyclohexanes cis-**11**, trans-**11** and trans-**14** could not inhibit the Ca^{2+} influx. Obviously, these three compounds do not behave like the σ_1 agonist opipramol.

The σ_1 antagonistic effect of the test compounds was next investigated by reverting the σ_1 agonistic effect of opipramol on these cells. For this purpose, the test compounds ($c = 10$ nM) were co-incubated with opipramol ($c = 100$ μM) and, subsequently, the Ca^{2+} influx was stimulated with KCl. With exception of cis-**11**, both trans-configured compounds trans-**11** and trans-**14** reduced the σ_1 agonistic effect of opipramol almost completely (Fig. 8). Obviously, both compounds behaved as σ_1 receptor antagonists in this assay. The low activity of cis-**11**, the ligand with the highest σ_1 affinity, was unexpected. We assume that a higher concentration of cis-**11** is required to antagonize the opipramol effect in this assay.

6. Inhibition of tumor cell growth

Next, the inhibition of tumor cell growth by stereoisomeric benzylamines **11** and phenylpiperazines **15** was investigated. The androgen negative human prostate cancer cell line DU145[54] was selected to evaluate the antiproliferative properties of the amines **11** and **15**. In brief, approximately 2000 cells were seeded in a 96-well plate and 24 h later, the test compounds were added in a concentration of 10 μM. After 72 h, the cells were fixed and proliferation/survival of the cells was evaluated by staining with Sulforhodamine B.[55].

The racemic cis-configured benzylamine cis-**11** as well as its enantiomers (1R,3S)-**11** and (1S,3R)-**11** showed significant antiproliferative effects on the DU145 prostate cancer cells (Fig. 9A). The trans-configured benzylamine (1R,3R)-**11** and (1S,3S)-**11** and the phenylpiperazines trans-**15** and cis-**15**, could not inhibit the growth of the tumor cells at the tested concentration of 10 μM. Thus, cis-**11** as well as its enantiomers (1R,3S)-**11** and (1S,3R)-**11** could represent promising candidates for further development in therapeutic targeting of human tumor cells.

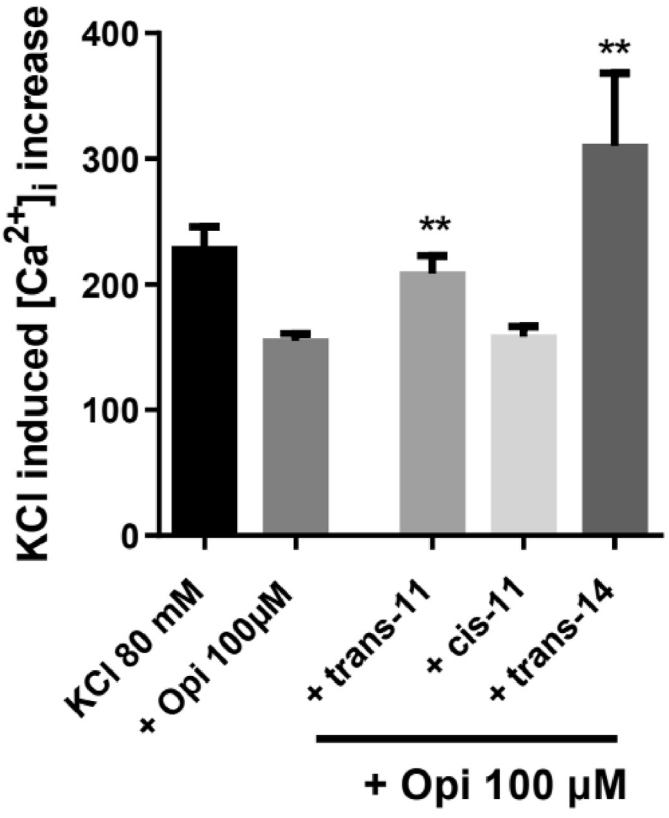

Fig. 8. Reversion of the effect of the σ_1 agonist opipramol on the Ca^{2+} influx in retinal ganglion cells by the σ_1 antagonists trans-**11**, cis-**11** and trans-**14**.

The activity of cis-**11** was evaluated in additional cancer cell lines under the same conditions (Fig. 9B). Both prostate (PC3 and 22RV1) and lung (H358, H441 and H522) cancer cell lines were sensitive to the antiproliferative effects of cis-**11**. Interestingly, the growth inhibitory activity of cis-**11** was comparable to that of the known σ_1 antagonist NE-100 tested under similar conditions (Fig. 9C).

7. Pharmacokinetic properties

7.1. Determination of the $logD_{7.4}$ value

The lipophilicity of a drug has a strong impact on various pharmacokinetic parameters. In particular, it has a strong influence on solubility [56,57], membrane and blood-brain-barrier penetration [58,59] and extent of biotransformation [60,61]. The lipophilicity can be described by the distribution coefficient at a specific pH value ($logD_{pH}$). In general, the physiological pH value of 7.4 is chosen. Very recently, we have reported on a micro shake flask method, which requires less than 1 mg of compound for the determination of $logD_{7.4}$ values, since the amount of drug in the buffer layer is determined by MS [62,63]. This method led to an experimentally determined $logD_{7.4}$ value of 3.23 ± 0.02 (±SEM, n = 9) for the most potent σ_1 receptor ligand (1R,3S)-**11** of this set of compounds. The experimentally determined $logD_{7.4}$ value of the trans-configured diastereomer (1S,3S)-**11** is in the same range ($logD_{7.4}$ = 3.34 ± 0.03 (±SEM, n = 9) showing that the relative configuration (cis or trans) did only slightly modulate the polarity of the corresponding molecules. Both $logD_{7.4}$ values are in a good range regarding barrier penetration.

7.2. Biotransformation of (1R,3S)-11

At first the metabolic stability of (1R,3S)-**11** was determined in vitro. For this purpose, (1R,3S)-**11** was incubated with mouse liver microsomes and NADPH. Mouse liver microsomes were chosen, since it was planned to test the σ_1 receptor ligand (1R,3S)-**11** in mice. After an incubation period of 90 min at 37 °C, 43 ± 1.6% (SD, n = 3) of the parent compound (1R,3S)-**11** remained unchanged. Although (1R,3S)-**11** is more stable than the reference compound imipramine (12 ± 1.7% (SD, n = 3) intact parent), more than 50% of (1R,3S)-**11** were transformed after 90 min.

In order to identify metabolic soft spots of the σ_1 receptor ligand (1R,3S)-**11**, metabolite structure elucidation was carried out by means of different LC-MS methods and with the use of collision-induced dissociation (CID). After incubation with mouse liver microsomes and NADPH, nine metabolites were identified (Scheme 3). Oxidation of the phenyl or cyclohexyl moiety led to phenol **11A** and cyclohexanol **11B**, respectively. Oxidation adjacent to the amino moiety resulted in the amide **11C** and the primary amine **11D** was formed by oxidative N-debenzylation. Further oxidation of cyclohexanol **11B** provided cyclohexanone **11**F. The catechol metabolite **11E** and the phenolamide metabolite **11G** were formed by oxidation at two different positions. The most interesting metabolites are the dimers **11H** and the glutathione adduct **11K**, the last being formed with and without addition of additional glutathione to the incubation mixture. The structures of the dimers **11H** and the glutathione adduct **11K** were elucidated by different experiments (see Section 5 "Biotransformation of (1R,3S)-**11**" in Supporting Information).

In order to analyze the pathway of metabolite formation, the phenol metabolite **11A** and the catechol metabolite **11E** were isolated and again incubated with mouse liver microsomes and NADPH. Upon incubation of phenol **11A** the metabolites **11E**, 11G, **11H**, and **11K** were formed, but incubation of catechol **11E** led only to **11K** (Figure S6). Therefore, the following pathway is postulated: at first phenol **11A** is oxidized to give a reactive epoxide, which is either trapped by another phenol **11A** to form the regioisomeric dimers **11H** or rearranged into catechol **11E**. Then, catechol 11E will be oxidized to form an *o*-quinone, which is trapped by glutathione to afford the glutathione adduct **11K** (Figure S7).

8. Conclusion

Replacement of the O-atoms of the acid labile acetalic 1,3-dioxane ring of the potent σ_1 receptor antagonist **1a** by two CH_2 moieties led to novel cyclohexane-based σ_1 receptor ligands **10**–**15**. The highest σ_1 receptor affinity was detected for the benzylamines **11**, which behaved as σ_1 antagonists in the Ca^{2+} influx assay using retinal ganglion cells. The cis-configured benzylamines (1R,3S)-**11** (K_i = 0.61 nM) and (1S,3R)-**11** (K_i = 1.3 nM) exhibited even higher σ_1 affinity than the 1,3-dioxane **1a** (K_i = 6.0 nM). Although the cyclohexane derivatives **11** are less polar than the 1,3-dioxane derivative **1a**, the $logD_{7.4}$ value experimentally determined for (1R,3S)-**11** ($logD_{7.4}$ = 3.13) lies in a promising range for penetration of physiological (i.e., cellular and blood-brain) barriers.

Separation of stereoisomeric primary alcohols **7** by chiral HPLC provided diastereomerically and enantiomerically pure amines. However, neither the relative nor the absolute configuration had a great influence on the σ_1 receptor affinity and selectivity. Whereas primary amines **10** and tertiary amines **13** and **15** show low to moderate σ_1 affinity, the secondary benzylamines **11** interact with high affinity with σ_1 receptors (K_i = 0.61–1.8 nM). Molecular dynamics simulations starting with the recently reported X-ray crystal structure of the σ_1 receptor showed very small differences in the free energy of binding for the four stereoisomeric benzylamines

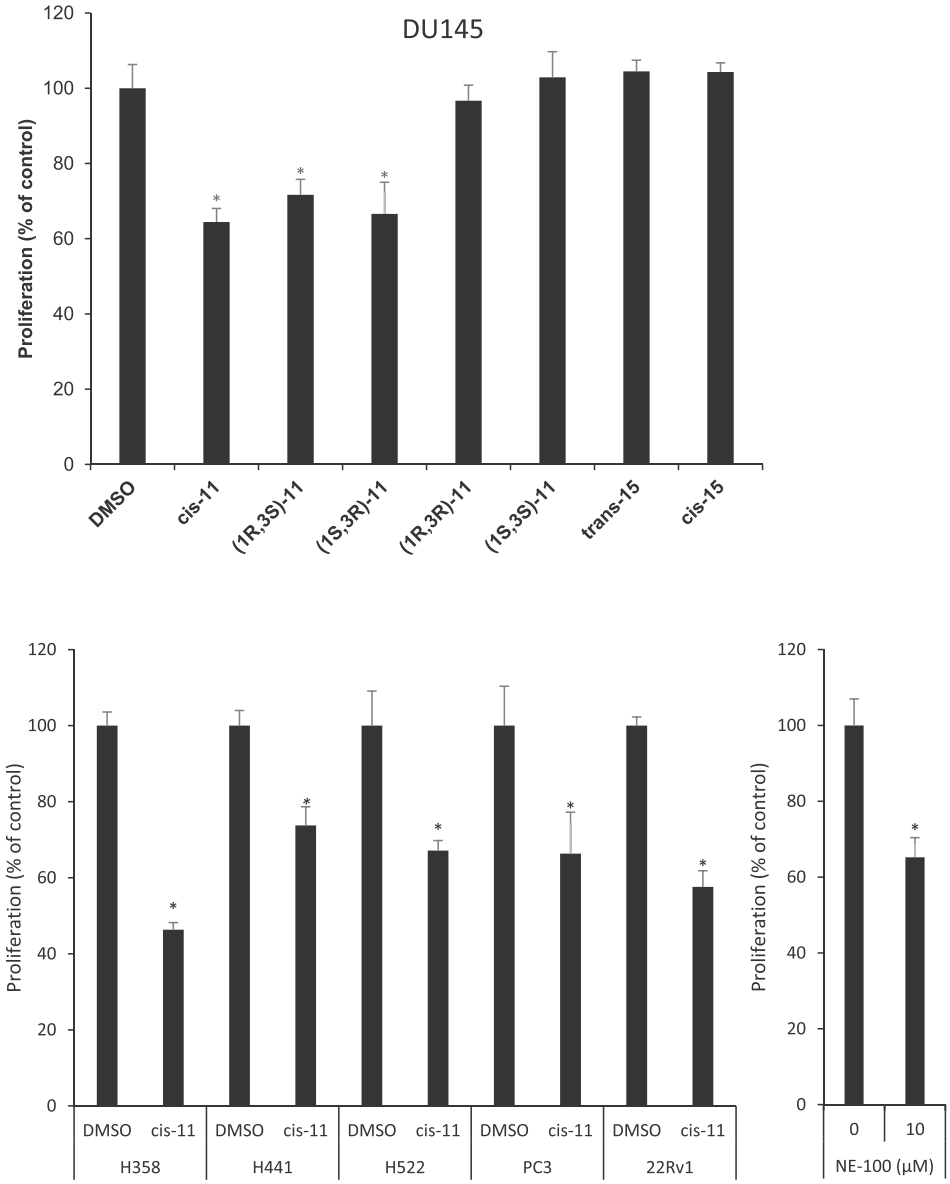

Fig. 9. A. Growth inhibition of human prostate tumor cells DU145 by stereoisomeric benzylamines **11** and phenylpiperazines **15** compared to DMSO. B. Antiproliferative activity of cis-**11** in various human cancer cells. C. growth inhibition of PC3 cells by NE-100.

11 in agreement with the corresponding experimental evidences. All compounds form a central polar interaction with E172 and bind to three receptor hydrophobic pockets. However, the different σ_1 affinity of aminoethylcyclohexanes with various N-substituents was attributed to different interactions with I124 forming optimal interactions with the benzyl moiety of **11** and least interactions with the primary amino group of **10**.

At a concentration of 10 μM, the two cis-configured benzylamines (1R,3S)-**11** and (1S,3R)-**11** as well as the racemic mixture cis-**11** displaying the highest σ_1 affinity of this series of compounds reduced the growth of DU145 cells, a highly aggressive prostate cancer cell line chosen for the initial compounds screening. The corresponding trans-configured diastereomers (1R,3R)-**11** and (1S,3S)-**11** and the phenylpiperazines cis-**15** and trans-**15** were not active in this assay. Importantly, the antiproliferative activity of cis-**11** was seen in additional human cancer cell lines, giving confidence on the reproducibility of the results. Due to the promising results, the metabolic stability of (1R,3S)-**11** was investigated. After incubation with mouse liver microsomes and NADPH for 90 min, 43% of unchanged parent compound were detected. Altogether, nine phase I and phase II metabolites were found including the glutathione adduct **11k**.

9. Experimental

9.1. Chemistry, general

Unless otherwise noted, moisture sensitive reactions were conducted under dry nitrogen. CH_2Cl_2 was distilled over CaH_2. THF was distilled over sodium/benzophenone. Et_2O and toluene were dried over molecular sieve 0.4 Å. Thin layer chromatography (tlc): Silica gel 60 F254 plates (Merck). Flash chromatography (fc): Silica gel 60, 40–64 μm (Merck); parentheses include: diameter of the column (d), length of the stationary phase, fraction size (V), eluent. Melting point: Melting point apparatus Mettler Toledo MP50 Melting Point System, uncorrected. MS: microOTOF-Q II (Bruker

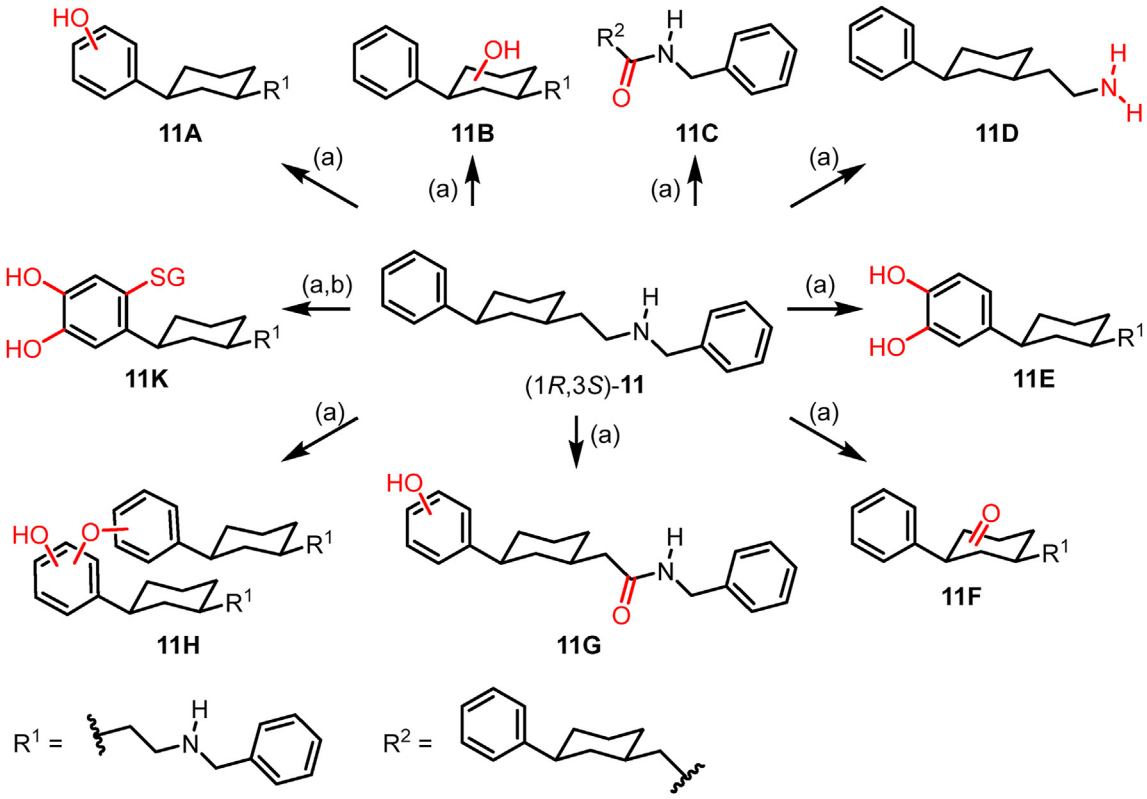

Scheme 3. Postulated and identified structures of phase I and phase II metabolites of σ_1 receptor antagonist (1R,3S)-**11** produced in vitro: (a) mouse liver microsomes and NADPH, (b) mouse liver microsomes, NADPH and glutathione (GSH).

Daltonics); APCI, atmospheric pressure chemical ionization. IR: FT-IR spectrophotometer MIRacle 10 (Shimadzu) equipped with ATR technique. Circular dichroism spectroscopy: JASCO J-600 spectropolarimeter (Jasco, Groβ-Umstadt), 0.1 cm cell, solvent CH3CN. Nuclear magnetic resonance (NMR) spectra were recorded on Agilent 600-MR (600 MHz for ^{1}H, 151 MHz for ^{13}C) or Agilent 400-MR spectrometer (400 MHz for ^{1}H, 101 MHz for ^{13}C); δ in ppm related to tetramethylsilane and measured referring to $CHCl_3$ (δ = 7.26 ppm (^{1}H NMR) and δ = 77.2 ppm (^{13}C NMR)), CHD_2OD (δ = 3.31 ppm (^{1}H NMR) and δ = 49.0 ppm (^{13}C NMR)) and DMSO-d_6 (δ = 2.54 ppm (^{1}H NMR) and δ = 39.5 ppm (^{13}C NMR)); coupling constants are given with 0.5 Hz resolution; the assignments of ^{13}C and ^{1}H NMR signals were supported by 2-D NMR techniques where necessary.

9.2. HPLC equipment and methods

9.2.1. HPLC equipment

Set 1: Pump L-7150, autosampler L-7200, UV-detector L-7400, interface D-7000, data transfer D-line, data acquisition: HSM-software (all Merck Hitachi).
Set 2: Pump L-7100, degasser L-7614, autosampler L-7200, UV-detector L-7400, interface D-7000, data transfer D-line, data acquisition: HSM-software (all Merck Hitachi).

9.2.2. 9.2.2. HPLC method A (preparative separation of cis/trans-diastereomers)

Equipment Set 1; column Phenomenex Gemini, 5 μm, C18, 110A, 250 mm/21.2 mm; guard column Phenomenex Gemini, 5 μm, C18, 110A, 50 mm/21.2 mm; flow rate 12 mL/min; detection wavelength 235 nm. Different solvents were used to separate different amines.

Method A1 for separation of cis-11 and trans-11: CH3CN:H2O = 55:45 + 0.1% NEt3.
Method A2 for separation of cis-15 and trans-15: CH3CN:H2O = 60:40 + 0.1% NEt3.
Method A3 for separation of cis-14 and trans-14: CH3OH:H2O = 70:30 + 0.1% NEt3.

9.2.3. 9.2.3. HPLC method B (chiral preparative separation of all four stereoisomers of 7)

Equipment: Set 1; column Daicel Chiralpak IB, 5 μm, 250 mm/20 mm; guard column Daicel Chiralpak IB, 5 μm, 20 mm/10 mm; flow rate 19 mL/min; detection wavelength 210 nm; solvent isohexane: isopropanol = 98 : 2.

9.2.4. 9.2.4. HPLC method C (separation of enantiomerically pure pairs of diastereomeric alcohols 7)

Equipment Set 1; column: Daicel Chiralpak IB, 5 μm, 250 mm/20 mm; guard column Daicel Chiralpak IB, 5 μm, 20 mm/10 mm; flow rate 20 mL/min; detection wavelength 210 nm; solvent isohexane: isopropanol = 98 : 2..

9.2.5. 9.2.5. HPLC method D (separation of diastereomeric benzylamines 11)

Equipment Set 1; column Phenomenex Gemini, 5 μm, C18, 110A, 250 mm/21.2 mm; guard column Phenomenex Gemini, 5 μm, C18, 110A, 50 mm/21.2 mm; flow rate 20 mL/min; detection wavelength 210 nm; solvent CH3CN: H2O = 65 : 35 + 2.0% NH3.

9.2.6. 9.2.6. HPLC method E (analysis of purity)

Equipment Set 2; column: LiChrospher® 60 RP-select B, 5 μm, LiChroCART® 250 mm/4 mm cartridge; guard column: LiChrospher® 60 RP-select B, 5 μm, LiChroCART® 4 mm/4 mm cartridge, manu-CART® NT cartridge holder; flow rate 1.0 mL/min; injection volume 5 μL; detection wavelength 210 nm; solvent A: water with 0.05% (v/v) trifluoroacetic acid; solvent B: CH3CN with 0.05% (v/v) trifluoroacetic acid; gradient elution: (A %): 0–4 min: 90%, 4–29 min: 90 → 0%, 29–31 min: 0%, 31–31.5 min: 0 → 90%, 31.5–40 min: 90%. The purity of all compounds was determined by this method. The purity of all test compounds is higher than 95% (unless otherwise noted).

9.3. Synthetic procedures

9.3.1. 3-Phenylcyclohexanone (4)

A mixture of dioxane/1.5 M KOH = 3/1 was degassed for 30 min in an ultrasonic bath. Under N_2 $[Rh(cod)_2]BF_4$ (19 mg, 0.047 mmol) and phenylboronic acid (288 mg, 2.36 mmol) were suspended in the dioxane/KOH mixture (5 mL) and the mixture was stirred for 30 min at room temperature. Afterwards cyclohex-2-en-1-one (**3**) (0.15 mL, 1.56 mmol) was added dropwise and the mixture was heated to 90 °C for 4.5 h. After cooling down the reaction mixture was transferred to a separating funnel, brine (15 mL) was added and the mixture was extracted with CH_2Cl_2 (4 x 20 mL). The combined organic layers were dried (Na_2SO_4), filtered and concentrated in vacuo. The crude product was purified by flash column chromatography (Ø 2.5 cm, h 18 cm, 10 mL, cyclohexane:ethyl acetate = 7:1, R_f = 0.35). Pale yellow oil, yield 233 mg (86%). $C_{12}H_{14}O$ (174.2 g/mol). MS (ESI): *m/z* = 371 (2 M + Na^+), 271 (2 M − Ph), 197 (M + Na^+). IR: $\tilde{\nu}$ (cm^{-1}) = 2938, 2866 (C–H), 1708 (C=O), 753, 698 (C-H_{arom}). ^{1}H NMR ($CDCl_3$): δ (ppm) = 1.73–1.91 (m, 2H, cyclohexane), 2.06–2.19 (m, 2H, cyclohexane), 2.34–2.63 (m, 4H, CH_2COCH_2), 3.02 (tt, J = 11.8/3.8 Hz, 1H, PhCH), 7.21–7.26 (m, 3H, arom), 7.31–7.36 (m, 2H, arom).

9.3.2. Methyl (3-phenylcyclohexylidene)acetate (5)

Ph_3P=$CHCO_2CH_3$ (4.81 g, 14.4 mmol) was added to a solution of 3-phenylcyclohexanone (**4**, 982 mg, 5.64 mmol) in toluene (8 mL) and the mixture was heated to reflux for 17 h. The solvent was removed in vacuo and the residue was purified by flash column chromatography (Ø 6 cm, h 20 cm, 160 mL, cyclohexane:ethyl acetate = 10:1, R_f = 0.43). Pale yellow oil, yield 1.15 g (89%). Purity (HPLC method E): 99.7% (t_R = 23.5 min). $C_{15}H_{18}O_2$ (230.3 g/mol). MS (ESI): *m/z* = 253 (M + Na^+), 231 (M + H^+). IR: $\tilde{\nu}$ (cm^{-1}) = 2929 (C–H), 1714 (C=O), 1647 (C=C), 755, 698 (C-H_{arom}). ^{1}H NMR ($CDCl_3$): δ (ppm) = 1.45–1.74 (m, 2H, cyclohexane), 1.86–2.10 (m, 3H, cyclohexane), 2.16–2.26 (m, 0.53H, 2-H_{ax} (E)), 2.30–2.49 (m, 1.47H, cyclohexane), 2.64–2.76 (m, 1H, PhCH), 3.67 (s, 3 × 0.47H, OCH_3), 3.70 (s, 3 × 0.53H, OCH_3), 3.90 (d, broad, *J* = 13.6 Hz, 0.53H, 6-H_{eq} (E)), 4.02 (ddt, J = 13.3/3.6/1.8 Hz, 0.47H, 2-H_{eq} (Z)), 5.68 (t, *J* = 1.5 Hz, 0.53H, C=CH), 5.71 (t, *J* = 1.7 Hz, 0.47H, C=CH), 7.15–7.36 (m, 5H, arom). The ratio of the two isomers is (E)-5:(Z)-5 = 53:47.

9.3.3. Methyl cis- and trans-2-(3-phenylcyclohexyl)acetate (cis-6 and trans-6)

The α,β-unsaturated ester **5** (1.21 g, 5.25 mmol) was dissolved in CH_3OH (30 mL) and Pd/C (10%, 311 mg) was added. The mixture was stirred under H_2 (balloon) for 3 h 15 min at room temperature. The mixture was filtered through Celite® and the residue was washed with small amounts of CH_3OH. The filtrate was concentrated in vacuo and the residue was purified by flash column chromatography twice (1. Ø 5 cm, h 14 cm, 30 mL, cyclohexane:ethyl acetate = 10:1, R_f = 0.50, 2. Ø 8 cm, h 12 cm, 65 mL, cyclohexane:ethyl acetate = 25:1, R_f = 0.22). Colorless oil, yield 1.01 g (83%). Purity (HPLC method E): 95.1% (t_R = 22.5 min). $C_{15}H_{20}O_2$ (232.3 g/mol). MS (ESI): *m/z* = 255 (M + Na^+), 250 (M + NH_4^+), 233 (M + H^+). IR: $\tilde{\nu}$ (cm^{-1}) = 2922, 2852 (C–H), 1734 (C=O), 755, 698 (C-H_{arom}). ^{1}H NMR ($CDCl_3$): δ (ppm) = 1.03 (qd, J = 12.5/3.2 Hz, 0.75H, 4-H_{ax}-cyclohexane or 6-H_{ax}-cyclohexane cis), 1.19 (q, *J* = 12.1 Hz, 0.75H, 2-H_{ax}-cyclohexane cis), 1.31–2.12 (m, 9 × 0.25H, 7 × 0.75H, cyclohexane), 2.25 (dd, J = 14.8/6.9 Hz, 0.75H, $CH_2CO_2CH_3$ cis), 2.29 (dd, J = 14.8/7.1 Hz, 0.75H, $CH_2CO_2CH_3$ cis), 2.50–2.54 (m, 2 × 0.25H, $CH_2CO_2CH_3$ trans), 2.60 (tt, J = 12.0/3.0 Hz, 0.75H, PhCH cis), 2.74–2.81 (tt, J = 10.6/3.8 Hz, 0.25H, PhCH trans), 3.67 (s, 3 × 0.75H, OCH_3 cis), 3.70 (s, 3 × 0.25H, OCH_3 trans), 7.18–7.33 (m, 5H, arom). Ratio of cis-**6**:trans-**6** = 75:25.

9.3.4. cis- and trans-2-(3-Phenylcyclohexyl)ethan-1-ol (cis-7 and trans-7)

Under N_2 the ester cis-**6**/trans-**6** (136 mg, 0.59 mmol) was dissolved in THF (20 mL). Under ice cooling a 1 M $LiAlH_4$ solution in THF (0.61 mL, 0.61 mmol) was added dropwise and the mixture was stirred for 30 min at 0 °C. The ice cooling was removed and the reaction mixture was stirred for 2 h at room temperature. H_2O was added under ice cooling till the gas formation stopped and the mixture was heated to reflux for 30 min. The precipitate was filtered through Celite® and washed with ethyl acetate. The filtrate was concentrated in vacuo and the residue was purified by flash column chromatography (Ø 3 cm, h 16 cm, 10 mL, cyclohexane:ethyl acetate = 3:1, R_f = 0.32). Colorless oil, yield 109 mg (91%). Purity (HPLC method E): cis-7 71.7% (t_R = 20.6 min), trans-7 26.2% (t_R = 20.4 min). $C_{14}H_{20}O$ (204.3 g/mol). MS (ESI): *m/z* = 227 (M + Na^+). IR: $\tilde{\nu}$ (cm^{-1}) = 3324 (O–H broad), 2918, 2850 (C–H), 753, 697 (C-H_{arom}). ^{1}H NMR ($CDCl_3$): δ (ppm) = 0.91 (qd, J = 12.5/3.0 Hz, 0.75H, 4-H_{ax}-cyclohexane or 6-H_{ax}-cyclohexane cis), 1.06 (q, *J* = 12.2 Hz, 0.75H, 2-H_{ax}-cyclohexane cis), 1.12–1.98 (m, 11 × 0.25H, 9 × 0.75H, cyclohexane, CH_2CH_2OH), 2.47 (tt, J = 11.9/3.2 Hz, 0.75H, PhCH cis), 2.69 (tt, J = 10.4/4.4 Hz, 0.25H, PhCH trans), 3.64 (t, *J* = 6.7 Hz, 2 × 0.75H, CH_2OH cis), 3.64 (t, *J* = 6.9 Hz, 2 × 0.25H, CH_2OH trans), 7.08–7.24 (m, 5H, arom). A signal for the OH-group is not seen in the spectrum. Ratio of cis-**7**:trans-**7** = 75:25.^{13}C NMR ($CDCl_3$): δ (ppm) = 21.4, 29.8, 30.0, 33.9, 35.2, 38.0, 38.2 (7 × 0.25C, cyclohexane trans, CH_2CH_2OH trans), 26.5, 32.8, 34.1, 34.6, 40.3, 41.2, 44.3 (7 × 0.75C, cyclohexane cis, CH_2CH_2OH cis), 60.7 (0.75C, CH_2OH cis), 61.6 (0.25C, CH_2OH trans), 125.8 (0.25C, C-4 arom trans), 125.9 (0.75C, C-4 arom cis), 126.8 (2 × 0.75C, C-2, C-6 arom cis), 126.9 (2 × 0.25C, C-2, C-6 arom trans), 128.3 (2 × 0.25C, C-3, C-5 arom trans), 128.3 (2 × 0.75C, C-3, C-5 arom cis), 147.3 (0.25C, C-1 arom trans), 147.6 (0.75C, C-1 arom cis). The stereoisomers (1R,3S)-**7**, (1S,3R)-**7**, (1S,3S)-**7** and (1R,3R)-**7** were separated by preparative chiral HPLC (method B).

9.3.5. (1R,3S)-2-(3-Phenylcyclohexyl)ethan-1-ol ((1R,3S)-7)

Pale yellow oil. Purity (HPLC method E): 99.0% (t_R = 20.3 min). Ratio of the stereoisomers: (1R,3S)-**7**: (1S,3R)-**7**: (1S,3S)-**7**: (1R,3R)-**7** = 98.57 : 0.12: 0.02 : 1.29. Retention time: 23.0 min (HPLC method B). Specific rotation: $[\alpha]_D^{20}$ = +15.7 (c = 1.02; CH_2Cl_2).

9.3.6. (1S,3R)-2-(3-Phenylcyclohexyl)ethan-1-ol ((1S,3R)-7)

Pale yellow oil. Purity (HPLC method E): 99.5% (t_R = 20.3 min). Ratio of the stereoisomers: (1R,3S)-**7**: (1S,3R)-**7**: (1S,3S)-**7**: (1R,3R)-**7** = 0.10 : 99.41: 0.42 : 0.07. Retention time: 40.2 min (HPLC method B). Specific rotation: $[\alpha]_D^{20}$ = −15.7 (c = 1.02; CH_2Cl_2).

9.3.7. (1S,3S)-2-(3-Phenylcyclohexyl)ethan-1-ol ((1S,3S)-7)

Pale yellow oil. Purity (HPLC method E): 98.7% (t_R = 20.0 min). Ratio of the stereoisomers: (1R,3S)-**7**: (1S,3R)-**7**: (1S,3S)-**7**: (1R,3R)-

7 = 0.35 : 0.42: 99.01 : 0.22. Retention time: 37.7 min (HPLC method B). Specific rotation: $[\alpha]_D^{20} = +2.4$ (c = 0.84; CH_2Cl_2).

9.3.8. (1R,3R)-2-(3-Phenylcyclohexyl)ethan-1-ol ((1R,3R)-7)

Pale yellow oil. Purity (HPLC method E): 99.6% (t_R = 20.0 min). Ratio of the stereoisomers: (1R,3S)-**7**: (1S,3R)-**7**: (1S,3S)-**7**: (1R,3R)-**7** = 0.16 : 0.27: 0.03 : 99.54. Retention time: 21.4 min (HPLC method B). Specific rotation: $[\alpha]_D^{20} = -1.6$ (c = 0.84; CH_2Cl_2).

9.3.9. cis- and trans-1-(2-Azidoethyl)-3-phenylcyclohexane (cis-8 and trans-8)

Under N_2, $Zn(N_3)_2$ py_2 (154 mg, 0.50 mmol) and PPh_3 (359 mg, 1.37 mmol) were dissolved in toluene (dried with molecular sieves 4 Å, 14 mL). The alcohol cis-/trans-**7** (134 mg, 0.66 mmol) was also dissolved in a small amount of toluene (dried with molecular sieves 4 Å) and the solution was added to the reaction mixture. Under ice cooling diisopropyl azodicarboxylate (DIAD, 0.26 mL, 1.32 mmol) was added dropwise, the ice bath was removed and the mixture was stirred at room temperature for 6 h. The solvent was evaporated in vacuo and the residue was purified by flash column chromatography (Ø 4.5 cm, h 17 cm, 30 mL, cyclohexane:ethyl acetate = 15:1, R_f = 0.70). Pale yellow oil, yield 110 mg (73%). Purity (HPLC method E): cis-8 72.3% (t_R = 24.2 min), trans-8 23.3% (t_R = 24.0 min). $C_{14}H_{19}N_3$ (229.3 g/mol). MS (APCI): *m/z* = 202 ($M - N_2 + H^+$). IR: $\tilde{\nu}$ (cm^{-1}) = 2921, 2852 (C—H), 2091 (N═N═N), 754, 698 (C-H_{arom}). ^{1}H NMR ($CDCl_3$): δ (ppm) = 0.85—0.95 (m, 0.75H, cyclohexane cis), 1.05 (q, *J* = 12.3 Hz, 0.75H, 2-H_{ax}-cyclohexane cis), 1.19—1.93 (m, 11 × 0.25H, 9 × 0.75H, cyclohexane, $CH_2CH_2N_3$), 2.48 (tt, J = 11.9/3.0 Hz, 0.75H, PhCH cis), 2.67 (tt, J = 10.5/3.9 Hz, 0.25H, PhCH trans), 3.25 (t, *J* = 6.9 Hz, 2 × 0.75H, CH_2N_3 cis), 3.25 (t, *J* = 7.2 Hz, 2 × 0.25H, CH_2N_3 trans), 7.09—7.25 (m, 5H, arom). Ratio of cis-**8**:trans-**8** = 75:25.

9.3.10. cis- and trans-[2-(3-Phenylcyclohexyl)ethyl] methanesulfonate (cis-9 and trans-9)

Under N_2 the alcohol cis-**7**/trans-**7** (1.16 g, 5.68 mmol) was dissolved in CH_2Cl_2 (20 mL). NEt_3 (2.37 mL, 17.03 mmol) was added and the mixture was stirred for 10 min under ice cooling. Methanesulfonyl chloride (0.66 mL, 8.51 mmol) was added dropwise and the mixture was stirred for 22 h at room temperature. The mixture was transferred into a separating funnel and the organic layer was washed with 0.5 M NaOH (2 x), 2 M NaOH (1 x) and a saturated solution of NH_4Cl (1 x). The combined aqueous layers were extracted with CH_2Cl_2 (2 x 20 mL).The combined organic layers were dried (Na_2SO_4), filtered and the solvent was removed in vacuo. The resulting product was purified by flash column chromatography (Ø 6 cm, h 17 cm, 30 mL, cyclohexane:ethyl acetate = 3:1, R_f = 0.42). Pale yellow solid, mp 40 °C, yield 1.36 g (85%). Purity (HPLC method E): cis-9 75.4% (t_R = 22.0 min), trans-9 24.5% (t_R = 21.8 min). $C_{15}H_{22}O_3S$ (282.4 g/mol). MS (ESI): *m/z* = 305 ($M + Na^+$). IR: $\tilde{\nu}$ (cm^{-1}) = 2920, 2851 (C—H), 1351, 1171 (O-mesyl), 756, 700 (C-H_{arom}). ^{1}H NMR ($CDCl_3$): δ (ppm) = 0.85—0.97 (m, 0.75H, cyclohexane cis), 1.08 (q, *J* = 12.2 Hz, 0.75H, 2-H_{ax}-cyclohexane cis), 1.18—2.00 (m, 11 × 0.25H, 9 × 0.75H, cyclohexane, CH_2CH_2O), 2.48 (tt, J = 11.9/3.0 Hz, 0.75H, PhCH cis), 2.63—2.71 (m, 0.25H, PhCH trans), 2.92 (s, 3 × 0.25H, OSO_2CH_3 trans), 2.93 (s, 3 × 0.75H, OSO_2CH_3 cis), 4.20—4.24 (m, 2H, $CH_2OSO_2CH_3$), 7.10—7.25 (m, 5H, arom). Ratio of cis-**9**:trans-**9** = 75:25.

9.3.11. {2-[(1R,3S)-3-Phenylcyclohexyl]ethyl} methanesulfonate ((1R,3S)-9)

The alcohol (1R,3S)-**7** (72 mg, 0.35 mmol) was dissolved in CH_2Cl_2 (10 mL) under N_2. NEt_3 (0.15 mL, 1.05 mmol) was added under ice cooling and the mixture was stirred for 10 min at 0 °C. Then methanesulfonyl chloride (0.04 mL, 0.52 mmol) was added, the ice bath was removed and the solution was stirred at room temperature overnight. The mixture was transferred into a separating funnel and washed with 0.5 M NaOH (2 x) and with a saturated solution of NH_4Cl (1 x). The organic layer was dried (Na_2SO_4), filtered and the solvent was removed under reduced pressure. The residue was purified by flash column chromatography (Ø 2.5 cm, h 15 cm, 10 mL, cyclohexane:ethyl acetate = 3:1). Colorless solid, mp 52 °C, yield 91 mg (92%). Purity (HPLC method E): 99.7% (t_R = 21.6 min). Specific rotation: $[\alpha]_D^{20} = +29.8$ (c = 1.45; CH_2Cl_2). Further analytical data see diastereomeric mixture cis-**9** and trans-**9**.

9.3.12. {2-[(1S,3R)-3-Phenylcyclohexyl]ethyl} methanesulfonate ((1S,3R)-9)

As described for (1R,3S)-**9**, a solution of (1S,3R)-**7** (85 mg, 0.42 mmol), NEt_3 (0.17 mL, 1.25 mmol) and methanesulfonyl chloride (0.05 mL, 0.63 mmol) in CH_2Cl_2 (10 mL) was stirred at room temperature overnight. The residue was purified by flash column chromatography (Ø 2.5 cm, h 19 cm, 10 mL, cyclohexane:ethyl acetate = 3:1). Colorless solid, mp 52 °C, yield 108 mg (91%). Purity (HPLC method E): 99.8% (t_R = 21.6 min). Specific rotation: $[\alpha]_D^{20} = -29.7$ (c = 1.45; CH_2Cl_2). Further analytical data see diastereomeric mixture cis-**9** and trans-**9**.

9.3.13. {2-[(1S,3S)-3-Phenylcyclohexyl]ethyl} methanesulfonate ((1S,3S)-9)

As described for (1R,3S)-**9**, a solution of (1S,3S)-**7** (25 mg, 0.12 mmol), NEt_3 (0.05 mL, 0.36 mmol) and methanesulfonyl chloride (0.01 mL, 0.18 mmol) in CH_2Cl_2 (5 mL) was stirred at room temperature for 5 h. The residue was purified by flash column chromatography (Ø 2.5 cm, h 15 cm, 10 mL, cyclohexane:ethyl acetate = 3:1). Pale yellow oil, yield 30 mg (87%). Purity (HPLC method E): 99.4% (t_R = 21.8 min). Specific rotation: $[\alpha]_D^{20} = -1.4$ (c = 1.04; CH_2Cl_2). Further analytical data see diastereomeric mixture cis-**9** and trans-**9**.

9.3.14. {2-[(1R,3R)-3-Phenylcyclohexyl]ethyl} methanesulfonate ((1R,3R)-9)

As described for (1R,3S)-**9**, a solution of (1R,3R)-**7** (24 mg, 0.12 mmol), NEt_3 (0.05 mL, 0.35 mmol) and methanesulfonyl chloride (0.01 mL, 0.18 mmol) in CH_2Cl_2 (5 mL) was stirred at room temperature for 4 h. The residue was purified by flash column chromatography (Ø 2.5 cm, h 17 cm, 10 mL, cyclohexane:ethyl acetate = 3:1). Pale yellow oil, yield 31 mg (92%). Purity (HPLC method E): 99.9% (t_R = 21.8 min). Specific rotation: $[\alpha]_D^{20} = +1.4$ (c = 1.04; CH_2Cl_2). Further analytical data see diastereomeric mixture cis-**9** and trans-**9**.

9.3.15. cis- and trans-2-(3-Phenylcyclohexyl)ethanamine (cis-10 and trans-10)

Pd/C (10%, 16 mg) was added to a solution of the azide cis-/trans-**8** (53 mg, 0.23 mmol) in CH_3OH (12 mL). The mixture was stirred under H_2 (balloon) for 2 h at room temperature. The mixture was filtered and the solvent removed in vacuo. The crude product was purified by flash column chromatography twice (1. Ø 2 cm, h 15 cm, 8 mL, CH_2Cl_2:CH_3OH = 1:1, R_f = 0.10, 2. Ø 1 cm, h 15 cm, 5 mL, CH_2Cl_2:CH_3OH = 1:1). Yellow oil, yield 15 mg (32%). Purity (HPLC method E): cis-10 81.4% (t_R = 16.3 min), trans-10 16.3% (t_R = 16.2 min). $C_{14}H_{21}N$ (203.3 g/mol). MS (ESI): *m/z* = 204 ($M + H^+$). IR: $\tilde{\nu}$ (cm^{-1}) = 2919, 2848 (C—H), 753, 698 (C-H_{arom}). ^{1}H NMR ($CDCl_3$): δ (ppm) = 0.90—1.00 (m, 0.75H, cyclohexane cis), 1.11 (q, *J* = 12.1 Hz, 0.75H, 2-H_{ax}-cyclohexane cis), 1.25—1.95 (m, 11 × 0.25H, 9 × 0.75H, cyclohexane, CH_2CH_2N), 2.53 (tt, J = 11.8/

3.1 Hz, 0.75H, PhCH cis), 2.73–2.80 (m, 3 × 0.25H, 2 × 0.75H, CH_2NH_2, PhCH trans), 7.11–7.31 (m, 5H, arom). Ratio of cis-**10**:trans-**10** = 75:25.^{13}C NMR ($CDCl_3$): δ (ppm) = 21.4, 30.0, 30.8, 33.8, 36.1, 38.0 (6 × 0.25C, cyclohexane trans, CH_2CH_2N trans), 26.5, 32.8, 34.1, 35.6, 39.5, 41.2 (6 × 0.75C, cyclohexane cis, CH_2CH_2N cis), 38.1 (0.25C, CH_2NH_2 trans), 40.5 (0.25C, PhCH trans), 41.2 (0.75C, CH_2NH_2 cis), 44.3 (0.75C, PhCH cis), 125.7 (0.25C, C-4 arom trans), 125.8 (0.75C, C-4 arom cis), 126.7, 128.3 (4 × 0.75C, arom cis), 126.9, 128.2 (4 × 0.25C, arom trans), 147.4 (0.25C, C-1 arom trans), 147.6 (0.75C, C-1 arom cis).

9.3.16. 2-[(1R,3S)-3-Phenylcyclohexyl]ethanamine ((1R,3S)-10)

A solution of the benzylamine (1R 3S)-**11** (40 mg, 0.14 mmol) in THF (12 mL) was filled in a pressure vessel. Pd/C (10%, 16 mg) was added and the mixture was placed in a hydrogenation apparatus. The solution was stirred under H_2 under pressure (5 bar) for 27 h. Then it was filtered through Celite®, the residue was washed with ethyl acetate and the combined organic layers were concentrated in vacuo. The product was purified by flash column chromatography twice (1. Ø 1 cm, h 15 cm, 5 mL, CH_2Cl_2:CH3OH = 1:1, 2. Ø 1 cm, h 16 cm, 5 mL, CH_2Cl_2:CH_3OH = 1:1). Yellow oil, yield 13 mg (47%). Purity (HPLC method E): 94.0% (t_R = 16.7 min). MS (EM, APCI): *m/z* = calculated for $C_{14}H_{22}N$ (M + H^+) 204.1747, found 204.1758. Further analytical data see diastereomeric mixture cis-**10** and trans-**10**.

9.3.17. 2-[(1S,3R)-3-Phenylcyclohexyl]ethanamine ((1S,3R)-10)

As described for (1R,3S)-**10**, a mixture of the benzylamine (1S,3R)-**11** (24 mg, 0.08 mmol) and Pd/C (10%, 11 mg) in THF (12 mL) was reacted with H_2 under pressure (5 bar) for 25.5 h. The residue was purified by flash column chromatography (Ø 1 cm, h 13 cm, 5 mL, CH_2Cl_2:CH_3OH = 1:1). Pale yellow oil, yield 7 mg (44%). Purity (HPLC method E): 98.0% (t_R = 16.3 min). MS (EM, APCI): *m/z* = calculated for $C_{14}H_{22}N$ (M + H^+) 204.1747, found 204.1751. Further analytical data see diastereomeric mixture cis-**10** and trans-**10**.

9.3.18. 2-[(1S,3S)-3-Phenylcyclohexyl]ethanamine ((1S,3S)-10)

As described for (1R,3S)-**10**, a mixture of the benzylamine (1S,3S)-**11** (37 mg, 0.13 mmol) and Pd/C (10%, 22 mg) in THF (14 mL) was reacted with H_2 under pressure (5 bar) for 27 h. The residue was purified by flash column chromatography (Ø 1 cm, h 15 cm, 5 mL, CH_2Cl_2:CH_3OH = 1:1). Yellow oil, yield 21 mg (81%). Purity (HPLC method E): 92% (t_R = 16.4 min). MS (EM, APCI): *m/z* = calculated for $C_{14}H_{22}N$ (M + H^+) 204.1747, found 204.1748. Further analytical data see diastereomeric mixture cis-**10** and trans-**10**.

9.3.19. 2-[(1R,3R)-3-Phenylcyclohexyl]ethanamine ((1R,3R)-10)

As described for (1R,3S)-**10**, a mixture of the benzylamine (1R,3R)-**11** (36 mg, 0.12 mmol) and Pd/C (10%, 12 mg) in THF (12 mL) was reacted with H_2 under pressure (5 bar) for 26 h. The residue was purified by flash column chromatography (Ø 1 cm, h 14 cm, 5 mL, CH_2Cl_2:CH_3OH = 1:1). Yellow oil, yield 10 mg (40%). Purity (HPLC method E): 91% (t_R = 16.3 min). MS (EM, APCI): *m/z* = calculated for $C_{14}H_{22}N$ (M + H^+) 204.1747, found 204.1749. Further analytical data see diastereomeric mixture cis-10 and trans-**10**.

9.3.20. cis-N-Benzyl-2-(3-phenylcyclohexyl)ethanamine (cis-11) and trans-N-benzyl-2-(3-phenylcyclohexyl)ethanamine (trans-11)

Benzylamine (0.15 mL, 1.39 mmol) was added to a solution of cis/trans-**9** (131 mg, 0.46 mmol) in CH_3CN (10 mL) and the mixture was heated to reflux for 15 h. The solvent was removed in vacuo. The residue was dissolved in ethyl acetate and washed with 0.5 M NaOH (2 x). The combined NaOH-layers were extracted with ethyl acetate (1 x). The combined organic layers were dried (Na_2SO_4), filtered, concentrated in vacuo and the residue was purified by flash column chromatography (Ø 2.5 cm, h 15 cm, 10 mL, cyclohexane:ethyl acetate = 7:1 + 1% dimethylethylamine, R_f = 0.27). Pale yellow oil, yield 112 mg (83%). Purity (HPLC method E): 99.2% (t_R = 19.5 min). $C_{21}H_{27}N$ (293.5 g/mol). MS (ESI): *m/z* = 294 (M + H^+). IR: $\tilde{\nu}$ (cm^{-1}) = 2917, 2848 (C–H), 731, 696 (C-H_{arom}). The diastereomers cis-**11** and trans-**11** were separated by preparative HPLC (HPLC method A1).

9.3.21. cis-N-Benzyl-2-(3-phenylcyclohexyl)ethanamine (cis-11)

After separation by preparative HPLC method A1, the fractions containing cis-**11** were concentrated in vacuo to about 100 mL and extracted with CH_2Cl_2 (4 x). The combined organic layers were dried (Na_2SO_4), filtered and the solvent was evaporated under reduced pressure. Colorless oil. Purity (HPLC method E): 99.7% (t_R = 20.2 min). Retention time: 110 min (HPLC method A1). ^{1}H NMR ($CDCl_3$): δ (ppm) = 0.87 (qd, J = 12.5/3.0 Hz, 1H, 4-H_{ax}-cyclohexane or 6-H_{ax}-cyclohexane), 1.04 (q, *J* = 12.2 Hz, 1H, 2-H_{ax}-cyclohexane), 1.18–1.83 (m, 9H, cyclohexane, CH_2CH_2N), 2.45 (tt, J = 11.9/3.0 Hz, 1H, PhCH), 2.60 (t, *J* = 7.4 Hz, 2H, CH_2CH_2NH), 3.71 (s, 2H, $NHCH_2Ph$), 7.09–7.27 (m, 10H, arom). ^{13}C NMR ($CDCl_3$): δ (ppm) = 26.5, 32.9, 34.2, 36.1, 37.8, 41.2 (6C, cyclohexane, CH_2CH_2N), 44.3 (1C, PhCH), 47.1 (1C, CH_2CH_2NH), 54.1 (1C, $NHCH_2Ph$), 125.8 (1C, C-4 $arom_{(benzyl)}$), 126.8 (2C, arom), 126.9 (1C, C-4 $arom_{(benzene)}$), 128.1, 128.3, 128.4 (6C, arom), 140.4 (1C, C-1 $arom_{(benzyl)}$), 147.7 (1C, C-1 $arom_{(benzene)}$).

9.3.22. trans-N-Benzyl-2-(3-phenylcyclohexyl)ethanamine (trans-11)

After separation by preparative HPLC method A1, the fractions containing trans-**11** were concentrated in vacuo to about 40 mL and extracted with CH_2Cl_2 (4 x). The combined organic layers were dried (Na_2SO_4), filtered and the solvent was evaporated under reduced pressure. Colorless oil. Purity (HPLC method E): 99.4% (t_R = 20.0 min). Retention time: 102 min (HPLC method A1). ^{1}H NMR ($CDCl_3$): δ (ppm) = 1.18–1.88 (m, 11H, cyclohexane, CH_2CH_2N), 2.60 (t, *J* = 7.6 Hz, 2H, CH_2CH_2NH), 2.65–2.72 (m, 1H, PhCH), 3.74 (s, 2H, $NHCH_2Ph$), 7.08–7.26 (m, 10H, arom). ^{13}C NMR ($CDCl_3$): δ (ppm) = 21.4, 30.1, 31.3, 32.5, 33.9, 38.0 (6C, cyclohexane, CH_2CH_2N), 38.1 (1C, PhCH), 47.9 (1C, CH_2CH_2NH), 54.1 (1C, $NHCH_2Ph$), 125.7 (1C, C-4 $arom_{(benzyl)}$), 126.9 (3C, arom), 128.2, 128.3, 128.4 (6C, arom), 140.2 (1C, C-1 $arom_{(benzyl)}$), 147.4 (1C, C-1 $arom_{(benzene)}$).

9.3.23. N-benzyl-2-[(1R,3S)-3-phenylcyclohexyl]ethanamine ((1R,3S)-11)

As described for cis/trans-11, a solution of (1R,3S)-**9** (88 mg, 0.31 mmol) and benzylamine (0.10 mL, 0.93 mmol) in CH_3CN (10 mL) was heated to reflux for 23 h. The residue was purified by flash column chromatography (Ø 2.5 cm, h 17 cm, 10 mL, cyclohexane:ethyl acetate = 7:1 + 1% dimethylethylamine). Colorless oil, yield 77 mg (85%). Purity (HPLC method E): 99.0% (t_R = 19.5 min). Specific rotation: $[\alpha]_D^{20}$ = +27.4 (c = 0.99; CH_2Cl_2). Further analytical data see cis-11.

9.3.24. N-benzyl-2-[(1S,3R)-3-phenylcyclohexyl]ethanamine ((1S,3R)-11)

As described for cis/trans-**11**, a solution of (1S, 3R)-9 (77 mg, 0.27 mmol) and benzylamine (0.09 mL, 0.81 mmol) in CH_3CN (6 mL) was heated to reflux for 15 h. The residue was purified by flash column chromatography (Ø 2.5 cm, h 16 cm, 10 mL, cyclohexane:ethyl acetate = 7:1 + 1% dimethylethylamine). Colorless oil,

yield 66 mg (83%). Purity (HPLC method E): 99.3% (t_R = 19.5 min). Specific rotation: $[\alpha]_D^{20} = -27.3$ (c = 0.99; CH_2Cl_2). Further analytical data see cis-**11**.

9.3.25. N-benzyl-2-[(1S,3S)-3-phenylcyclohexyl]ethanamine ((1S,3S)-11)

As described for cis/trans-**11**, a solution of (1S, 3S)-9 (26 mg, 0.09 mmol) and benzylamine (0.03 mL, 0.27 mmol) in CH_3CN (8 mL) was heated to reflux for 23 h. The residue was purified by flash column chromatography (Ø 2.5 cm, h 15 cm, 10 mL, cyclohexane:ethyl acetate = 7:1 + 1% dimethylethylamine). Colorless oil, yield 22 mg (85%). Purity (HPLC method E): 97.5% (t_R = 19.4 min). Specific rotation: $[\alpha]_D^{20} = +8.3$ (c = 0.90; CH_2Cl_2). Further analytical data see trans-**11**.

9.3.26. N-benzyl-2-[(1R,3R)-3-phenylcyclohexyl]ethanamine ((1R,3R)-11)

As described for cis/trans-**11**, a solution of (1R,3R)-**9** (24 mg, 0.08 mmol) and benzylamine (0.03 mL, 0.25 mmol) in CH_3CN (8 mL) was heated to reflux for 23 h. The residue was purified by flash column chromatography (Ø 2.5 cm, h 16 cm, 10 mL, cyclohexane:ethyl acetate = 7:1 + 1% dimethylethylamine). Colorless oil, yield 21 mg (89%). Purity (HPLC method E): 95.1% (t_R = 19.3 min). Specific rotation: $[\alpha]_D^{20} = -8.3$ (c = 0.90; CH_2Cl_2). Further analytical data see trans-**11**.

9.3.27. cis- and trans-4-phenyl-N-[2-(3-phenylcyclohexyl)ethyl] butan-1-amine (cis-12 and trans-12)

After dissolving cis-**9**/trans-**9** (51 mg, 0.18 mmol) in CH_3CN (10 mL), 4-phenylbutan-1-amine (0.09 mL, 0.54 mmol) was added and the mixture was heated to reflux for 22 h. Then the solvent was evaporated in vacuo and ethyl acetate (15 mL) was added. The resulting suspension was washed with 0.5 M NaOH (2 x 5 mL). The organic layer was dried (Na_2SO_4), filtered, concentrated in vacuo and the residue was purified by flash column chromatography (Ø 2.5 cm, h 15 cm, 10 mL, CH_2Cl_2:CH_3OH = 4:1, R_f = 0.28). Pale yellow resin, yield 45 mg (75%). Purity (HPLC method E): 97.3% (t_R = 21.9 min). $C_{24}H_{33}N$ (335.5 g/mol). MS (ESI): *m/z* = 336 ($M + H^+$). MS (EM, APCI): *m/z* = calculated for $C_{24}H_{34}N$ ($M + H^+$) 336.2686, found 336.2694. IR: $\tilde{\nu}$ (cm^{-1}) = 2920, 2852 (C—H), 745, 697 (C-H_{arom}). ^{1}H NMR ($CDCl_3$): δ (ppm) = 0.89—1.00 (m, 0.75H, cyclohexane cis), 1.11 (q, *J* = 12.3 Hz, 0.75H, 2-H_{ax}-cyclohexane cis), 1.26—1.89 (m, 15 × 0.25H, 13 × 0.75H, cyclohexane, CH_2CH_2N, $PhCH_2CH_2CH_2$), 2.52 (tt, J = 11.9/3.1 Hz, 0.75H, PhCH cis), 2.60—2.80 (m, 7.25H, CH_2NHCH_2, CH_2Ph, PhCH trans), 7.15—7.30 (m, 10H, arom). Ratio of cis-**12**:trans-**12** = 75:25.^{13}C NMR ($CDCl_3$): δ (ppm) = 21.4, 29.2, 29.3, 30.1, 31.4, 32.1, 33.9, 35.8 (8 × 0.25C, cyclohexane trans, CH_2CH_2N trans, $CH_2CH_2CH_2CH_2$ trans), 26.5, 29.0, 29.1, 32.8, 34.1, 35.7, 36.1, 37.1 (8 × 0.75C, cyclohexane cis, CH_2CH_2N cis, $CH_2CH_2CH_2CH_2$ cis), 37.9 (0.25C, PhCH trans), 38.1 (0.25C, $PhCH_2$ trans), 41.1 (0.75C, PhCH cis), 44.3 (0.75C, $PhCH_2$ cis), 47.3 (0.75C, $NHCH_2$ cis), 48.3 (0.25C, $NHCH_2$ trans), 49.6 (0.75C, $NHCH_2$ cis), 49.7 (0.25C, $NHCH_2$ trans), 125.7, 125.8, 125.9, 126.8, 126.9, 128.2, 128.3, 128.4 (10C, arom), 142.2 (0.75C, C-1 arom cis), 142.3 (0.25C, C-1 arom trans), 147.3 (0.25C, C-1 arom trans), 147.6 (0.75C, C-1 arom cis).

9.3.28. cis- and trans-N,N-Dimethyl-2-(3-phenylcyclohexyl) ethanamine (cis-13 and trans-13)

The mesylate cis-**9**/trans-**9** (34 mg, 0.12 mmol) was dissolved in CH_3CN (6 mL) and transferred to a 10-mL microwave reaction vessel. A 2 M solution of dimethylamine in THF (0.18 mL, 0.36 mmol) was added. The microwave parameters were set as follows: Power (max.) 200 W; pressure (max.) 8 bar; temperature (max.) 140 °C; reaction time ramp time 5 min, hold time 15 min. After the microwave irradiation, the solvent was evaporated under reduced pressure and the crude product was purified by flash column chromatography (Ø 2 cm, h 18 cm, 8 mL, CH_2Cl_2:CH_3OH = 9.5:0.5 + 1% NEt_3, R_f = 0.33). Pale yellow resin, yield 22 mg (79%). Purity (HPLC method E): 97.1% (t_R = 18.0 min). $C_{16}H_{25}N$ (231.4 g/mol). MS (ESI): *m/z* = 232 ($M + H^+$). MS (EM, APCI): *m/z* = calculated for $C_{16}H_{26}N$ ($M + H^+$) 232.2060, found 232.2119. IR: $\tilde{\nu}$ (cm^{-1}) = 2920, 2852 (C—H), 2813, 2761 (N—C—H), 752, 697 (C-H_{arom}). ^{1}H NMR ($CDCl_3$): δ (ppm) = 0.85—0.94 (m, 0.75H, cyclohexane cis), 1.05 (q, *J* = 12.3 Hz, 0.75H, 2-H_{ax}-cyclohexane cis), 1.18—1.85 (m, 11 × 0.25H, 9 × 0.75H, cyclohexane, CH_2CH_2N), 2.20 (s, 6 × 0.75H, (tt, J = 11.9/3.0 Hz, 0.75H, PhCH cis), 2.64—2.73 (m, 0.25H, PhCH trans), 7.08—7.24 (m, 5H, arom). Ratio of cis-**13**:trans-**13** = 75:25.^{13}C NMR ($CDCl_3$): δ (ppm) = 21.4, 29.8, 30.0, 31.5, 33.9, 38.0 (6 × 0.25C, cyclohexane trans, CH_2CH_2N trans), 26.4, 32.9, 34.1, 35.0, 36.2, 41.2 (6 × 0.75C, cyclohexane cis, CH_2CH_2N cis), 38.2 (0.25C, PhCH trans), 44.3 (0.75C, PhCH cis), 45.3 (2 × 0.75C, $N(CH_3)_2$ cis), 45.3 (2 × 0.25C, $N(CH_3)_2$ trans), 57.3 (0.75C, $CH_2N(CH_3)_2$ cis), 58.3 (0.25C, $CH_2N(CH_3)_2$ trans), 125.7 (0.25C, C-4 arom trans), 125.8 (0.75C, C-4 arom cis), 126.8 (2 × 0.75C, C-2, C-6 arom cis), 126.9 (2 × 0.25C, C-2, C-6 arom trans), 128.2 (2 × 0.25C, C-3, C-5 arom trans), 128.3 (2 × 0.75C, C-3, C-5 arom cis), 147.4 (0.25C, C-1 arom trans), 147.6 (0.75C,C-1 arom cis).

9.3.29. N,N-Dimethyl-2-[(1R,3S)-3-phenylcyclohexyl]ethanamine ((1R,3S)-13)

Pd/C (10%, 9 mg) was added to a solution of benzylamine (1R,3S)-**11** (37 mg, 0.13 mmol) in CH_3OH (15 mL). HOAc (2 drops) was added and the mixture was stirred under H_2 (balloon) for 22.5 h. Additional Pd/C (10%, 9 mg) was added and the solution was again stirred under H_2 (balloon) for 6 h. Then it was filtered, the solvent was removed in vacuo and the residue was purified by flash column chromatography twice (1. Ø 1 cm, h 13 cm, 5 mL, CH_2Cl_2:CH_3OH = 9.5:0.5 + 1% dimethylethylamine, R_f = 0.33, 2. Ø 1 cm, h 16 cm, 5 mL, CH_2Cl_2:CH_3OH = 1:1, R_f = 0.30). Pale yellow oil, yield 15 mg (48%). Purity (HPLC method E): 96.8% (t_R = 17.0 min). MS (EM, APCI): *m/z* = calculated for $C_{16}H_{26}N$ ($M + H^+$) 232.2060, found 232.2052. Further analytical data see diastereomeric mixture cis-**13** and trans-**13**.

9.3.30. N,N-Dimethyl-2-[(1S,3R)-3-phenylcyclohexyl]ethanamine ((1S,3R)-13)

As described for (1R,3S)-**13**, a solution of (1S,3R)-**11** (37 mg, 0.13 mmol), Pd/C (10%, 10 mg) and HOAc (2 drops) in CH_3OH (15 mL) was stirred under H_2 (balloon) for 19.5 h. Addition of further Pd/C (10%) was not necessary. The residue was purified by flash column chromatography twice (1. Ø 1 cm, h 18 cm, 5 mL, CH_2Cl_2:CH_3OH = 9.5:0.5 + 1% dimethylethylamine, 2. Ø 1 cm, h 15 cm, 5 mL, CH_2Cl_2:CH_3OH = 1:1). Pale yellow oil, yield 9 mg (30%). Purity (HPLC method E): 96.1% (t_R = 17.0 min). MS (EM, APCI): *m/z* = calculated for $C_{16}H_{26}N$ ($M + H^+$) 232.2060, found 232.2048. Further analytical data see diastereomeric mixture cis-**13** and trans-**13**.

9.3.31. cis-1-[2-(3-Phenylcyclohexyl)ethyl]pyrrolidine (cis-14) and trans-1-[2-(3-Phenylcyclohexyl)ethyl]pyrrolidine (trans-14)

Pyrrolidine (0.18 mL, 2.18 mmol) was added to a solution of mesylate cis-**9**/trans-**9** (205 mg, 0.73 mmol) in CH_3CN (25 mL) and the mixture was heated to reflux for 25 h CH_3CN was removed in vacuo and the residue was dissolved in ethyl acetate (30 mL). The organic layer was washed with 0.5 M NaOH (2 x 10 mL). Due to slow phase separation more ethyl acetate was added. Afterwards the organic layer was dried (Na_2SO_4), filtered and concentrated in vacuo. The residue was purified by flash column chromatography

(Ø 2 cm, h 16 cm, 10 mL, CH_2Cl_2:CH_3OH = 9:1 + 1% NEt_3, R_f = 0.57). Pale yellow oil, yield 135 mg (72%). Purity (HPLC method E): 97.8% (t_R = 18.6 min). $C_{18}H_{27}N$ (257.4 g/mol). MS (ESI): *m/z* = 591 (2 M + Ph), 258 (M + H^+). IR: $\tilde{\nu}$ (cm^{-1}) = 2919, 2850 (C–H), 2782 (N–C–H), 754, 698 (C-H_{arom}). The diastereomers cis-**14** and trans-**14** were separated by preparative HPLC (HPLC method A3).

9.3.32. cis-1-[2-(3-Phenylcyclohexyl)ethyl]pyrrolidine (cis-14)

After separation by preparative HPLC method A3, the fractions containing cis-**14** were concentrated in vacuo to about 150 mL and extracted with CH_2Cl_2 (4 x). The combined organic layers were dried (Na_2SO_4), filtered and the solvent was evaporated under reduced pressure. Pale yellow oil. Purity (HPLC method E): 99.5% (t_R = 18.5 min). Retention time: 129 min (HPLC method A3). MS (EM, APCI): *m/z* = calculated for $C_{18}H_{28}N$ (M + H^+) 258.2216, found 258.2255.^{1}H NMR ($CDCl_3$): δ (ppm) = 0.85–0.94 (m, 1H, cyclohexane), 1.06 (q, *J* = 12.2 Hz, 1H, 2-H_{ax}-cyclohexane), 1.19–1.85 (m, 13H, cyclohexane, CH_2CH_2N, $N(CH_2CH_2)_2$), 2.39–2.45 (m, 6H, $CH_2N(CH_2CH_2)_2$), 2.50 (tt, J = 11.9/3.1 Hz, 1H, PhCH), 7.09–7.24 (m, 5H, arom). ^{13}C NMR ($CDCl_3$): δ (ppm) = 23.4 (2C, $N(CH_2CH_2)_2$, 26.5, 33.0, 34.2, 36.7, 41.3 (6C, cyclohexane, CH_2CH_2N), 44.4 (1C, PhCH), 54.2 (2C, $N(CH_2CH_2)_2$), 54.3 (1C, $CH_2N(CH_2CH_2)_2$), 125.8 (1C, C-4 arom), 126.8 (2C, C-2, C-6 arom), 128.3 (2C, C-3, C-5 arom), 147.7 (1C, C-1 arom).

9.3.33. trans-1-[2-(3-Phenylcyclohexyl)ethyl]pyrrolidine (trans-14)

After separation by preparative HPLC method A3, the fractions containing trans-**14** were concentrated in vacuo to about 40 mL and extracted with CH_2Cl_2 (4 x). The combined organic layers were dried (Na_2SO_4), filtered and the solvent was evaporated under reduced pressure. Pale yellow oil. Purity (HPLC method E): 96.7% (t_R = 18.4 min). Retention time: 118 min (HPLC method A3). MS (EM, APCI): *m/z* = calculated for $C_{18}H_{28}N$ (M + H^+) 258.2216, found 258.2259.^{1}H NMR ($CDCl_3$): δ (ppm) = 0.66–1.83 (m, 15H, cyclohexane, CH_2CH_2N, $N(CH_2CH_2)_2$), 2.38–2.47 (m, 6H, $CH_2N(CH_2CH_2)_2$), 2.66–2.74 (m, 1H, PhCH), 7.08–7.24 (m, 5H, arom). ^{13}C NMR ($CDCl_3$): δ (ppm) = 21.4, 29.7, 30.2, 31.9, 34.0, 38.0 (6C, cyclohexane, CH_2CH_2N), 23.4 (2C, $N(CH_2CH_2)_2$), 38.1 (1C, PhCH), 54.3 (2C, $N(CH_2CH_2)_2$), 55.3 (1C, $CH_2N(CH_2CH_2)_2$), 125.7 (1C, C-4 arom), 126.9 (2C, C-2, C-6 arom), 128.2 (2C, C-3, C-5 arom), 147.4 (1C, C-1 arom).

9.3.34. cis-1-Phenyl-4-[2-(3-phenylcyclohexyl)ethyl]piperazine (cis-15) and trans-1-phenyl-4-[2-(3-phenylcyclohexyl)ethyl] piperazine (trans-15)

To a solution of mesylate cis-**9**/trans-**9** (126 mg, 0.45 mmol) in CH_3CN (27 mL), 1-phenylpiperazine (0.20 mL, 1.34 mmol) was added and the mixture was heated to reflux for 27 h. Then the solvent was evaporated in vacuo, the residue was dissolved in ethyl acetate (40 mL) and the organic layer was washed with 0.5 M NaOH (2 x 10 mL). The organic layer was dried (Na_2SO_4), filtered, the solvent was removed in vacuo and the residue was purified by flash column chromatography (Ø 3.5 cm, h 15.5 cm, 10 mL, cyclohexane:ethyl acetate = 3:1, R_f = 0.61 (ethyl acetate)). Pale yellow resin, yield 140 mg (89%). $C_{24}H_{32}N_2$ (348.5 g/mol). MS (ESI): *m/z* = 349 (M + H^+). IR: $\tilde{\nu}$ (cm^{-1}) = 2919 (C–H), 2815 (N–C–H), 754, 697 (C-H_{arom}). The diastereomers cis-15 and trans-15 were separated by preparative HPLC (HPLC method A2).

9.3.35. cis-1-Phenyl-4-[2-(3-phenylcyclohexyl)ethyl]piperazine (cis-15)

After separation by preparative HPLC, CH_3CN of the fractions containing cis-**15** was removed and the residue was extracted with CH_2Cl_2 (4 x). The combined organic layers were dried (Na_2SO_4), filtered and the solvent was evaporated under reduced pressure. Colorless solid. Purity (HPLC method E): 99.3% (t_R = 21.0 min). Retention time: 139 min (HPLC method A2). MS (EM, APCI): *m/z* = calculated for $C_{24}H_{33}N_2$ (M + H^+) 349.2638, found 349.2659.^{1}H NMR ($CDCl_3$): δ (ppm) = 0.86–0.97 (m, 1H, cyclohexane), 1.07 (q, *J* = 12.2 Hz, 1H, 2-H_{ax}-cyclohexane), 1.19–1.48 (m, 5H, cyclohexane), 1.73–1.87 (m, 4H, cyclohexane, CH_2CH_2N), 2.37 (t, *J* = 7.1 Hz, 2H, CH_2CH_2N), 2.47 (tt, J = 11.9/3.0 Hz, 1H PhCH), 2.53 (t, *J* = 5.0 Hz, 4H, $CH_2N(CH_2CH_2)_2N$), 3.14 (t, *J* = 5.1 Hz, 4H, $N(CH_2CH_2)_2NPh$), 6.78 (tt, J = 7.3/0.8 Hz, 1H, $arom_{(phenylpiperazine)}$ para), 6.86 (dd, J = 8.7/0.9 Hz, 2H, $arom_{(phenylpiperazine)}$ ortho), 7.09–7.24 (m, 7H, arom).

9.3.36. trans-1-Phenyl-4-[2-(3-phenylcyclohexyl)ethyl]piperazine (trans-15)

After separation by preparative HPLC, CH_3CN of the fractions containing trans-**15** was removed and the residue was extracted with CH_2Cl_2 (4 x). The combined organic layers were dried (Na_2SO_4), filtered and the solvent was evaporated under reduced pressure. Pale brown oil. Purity (HPLC method E): 99.0% (t_R = 20.4 min). Retention time: 131 min (HPLC method A2). MS (EM, APCI): *m/z* = calculated for $C_{24}H_{33}N_2$ (M + H^+) 349.2638, found 349.2612.^{1}H NMR ($CDCl_3$): δ (ppm) = 1.40–1.85 (m, 11H, cyclohexane, CH_2CH_2N), 2.36 (t, *J* = 7.8 Hz, 2H, CH_2CH_2N), 2.56 (t, *J* = 4.8 Hz, 4H, $CH_2N(CH_2CH_2)_2N$), 2.68–2.75 (m, 1H, PhCH), 3.16 (t, *J* = 4.9 Hz, 4H, $N(CH_2CH_2)_2NPh$), 6.79 (t, *J* = 7.3 Hz, 1H, $arom_{(phenylpiperazine)}$ para), 6.87 (d, *J* = 8.4 Hz, 2H, $arom_{(phenylpiperazine)}$ ortho), 7.09–7.24 (m, 7H, arom).

9.4. Receptor binding studies

Experimental details for recording σ_1 and σ_2 receptor affinity [46–48] are given in the Supporting Information.

9.5. Computational details

The membrane-bound 3D structure of the σ_1 receptor was obtained starting from the available Protein Data Bank file (pdb code: 5HK1)[11] and following a procedure previously described [50,51]. The optimized structures of the new tested compounds were docked into each protein identified binding pocket using Autodock 4.2.6/Autodock Tools1.4.61[64] on a win64 platform. The resulting complex was further energy minimized to convergence. The intermolecular complex was then solvated by a cubic box of TIP3P water molecules [65] and energy minimized using a combination of molecular dynamics (MD) techniques [50,51]. 20 ns molecular dynamics (MD) simulations at 298 K were then employed for system equilibration, and further, 50-ns MD were run for data production. Following the MM/PBSA approach [52] each binding free energy values (ΔG_{bind}) were calculated as the sum of the electrostatic, van der Waals, polar solvation, nonpolar solvation, (ΔH_{bind}) and entropic contributions (TΔSbind). The PRBFED analysis was carried out using the Molecular Mechanics/Generalized Boltzmann Surface Area (MM/GBSA) approach [66] and was based on the same snapshots used in the binding free energy calculation. All simulations were carried out using the pmemd and pmemd.CUDA modules of Amber 18,[67] running on our own CPU/GPU calculation cluster. Molecular graphics images were produced using the UCSF Chimera package (v.1.14) [68]. All other graphs were obtained using GraphPad Prism (v. 6.0) [69].

9.6. Ca^{2+} influx assay, fluorescence measurements with fura-2-AM

Concentrations c ($Ca^{2+}{}_i$) were measured in single PC12 cells using the fluorescent indicator fura-2-AM in combination with a monochromator-based imaging system (FEI today Thermo Fisher Scientific, SCR_008452) attached to a fluid immersion objective.

Cells were loaded with 0.5 μM fura-2-AM and 0.01% Pluronic F-127 for 30 min at 37 °C in a standard solution composed of 138 mM NaCl, 6 mM KCl, 1 mM $MgCl_2$, 2 mM $CaCl_2$, 5.5 mM glucose, and 10 mM HEPES (adjusted to pH 7.4 with NaOH at 37 °C). Cover slips were then washed in fresh buffer for 30 min and mounted in a perfusion chamber on the stage of the microscope (Olympus EX51WI, Hamburg, Germany). For measurements of c (Ca^{2+}_i), cells were excited at 340 and 380 nm and emission was measured at 510 nm. After correction for background fluorescence, the fluorescence ratio F340/F380 of the emission was calculated. Fura-2-signals were calibrated according to the method of Grynkiewicz et al. [53], using a K_D value of 224 nM. 10–20 cells were measured on slide and at least two replicates/independent experiment were conducted. At least five independent experiments were measured.

9.7. Proliferation assay

Human prostate cancer cell lines (i.e., DU145, PC3 and 22Rv1) and lung cancer cell lines (i.e, H358, H441 and H522) were purchased from ATCC and maintained in adherent conditions in RPMI 1640 medium (21,875–034, Gibco®) supplemented with 2% (S)-glutamine, 10% fetal bovine serum (FBS) (10,437–036, Gibco®) and 1% penicillin-streptomycin (15,140–122, Gibco®). For the proliferation assays, the cells were seeded at a density of 1×10^3 (lung) or 2×10^3 (prostate) cells/well in 96-well tissue culture plates. 24 h later, the cells were treated with the compounds (10 μM) for 72 h. Then, the cells were fixed with 10% (w/v) trichloroacetic acid and stained with sulforhodamine B for 30 min. The excess of the dye was removed by washing repeatedly with 1% (v/v) acetic acid and the protein-bound dye was solubilized with Tris base solution for optical density (OD) measurement at 510 nm with a microplate reader. Cell proliferation and viability were expressed as percentages relative to those of DMSO treated cells. *$p \leq 0.05$.

9.8. $logD_{7.4}$ value determinatio [62]

MOPS (372.5 mg, 8.9 mM) and MOPS sodium salt (513.4 mg, 11.1 mM) were dissolved in H_2O (200 mL) to prepare 20 mM MOPS buffer with pH 7.4. n-octanol and MOPS buffer were saturated with each other by stirring a two-phase system for 24 h. The final concentration of DMSO was kept below 1% in all samples. The $logD_{7.4}$ values were determined using three different volume ratios of saturated buffer and saturated n-octanol (750 μL and 750 μL (1:1), 500 μL and 1000 μL (1:2), 1000 μL and 500 μL (2:1)). The 10 mM DMSO stock solution was diluted differently for each compound so that the intensities remained inside the linear range of the MS detector. The diluted DMSO stock solution was added to the buffer, afterwards n-octanol was added. The combined DMSO/buffer mixtures were pipetted into 2 mL safe lock tubes. Afterwards, the tubes were vortexed for 2 min and subsequently centrifuged at 20 °C with 16,000 rpm for 10 min (centrifuge 5427 R, Eppendorf™, Hamburg, Germany). An aliquot of the aqueous layer was analyzed by LC-MS (LC-SQ setup, method A). Each sample with one of the three ratios of buffer/n-octanol was prepared three times resulting in a total of nine experiments ($n = 9$). The calibration curve was prepared with MOPS buffer saturated with n-octanol to match the matrix of the samples, covering their concentration range. With the determined concentration in the buffer phase, the $logD_{7.4}$ value was calculated using equation 1 (p. 2).

9.9. Biotransformation studies

Experimental details on biotransformation studies are given in Supporting Information.

Supporting Information

The Supporting Information contains purity data of all compounds, chiral HPLC of the stereoisomeric alcohols 7, experimental procedures for receptor binding studies, in silico binding thermodynamics and per residue binding enthalpy, details on biotransformation studies, and ^1H and ^{13}C NMR spectra of prepared compounds.

Declaration of competing interest

The authors declare that they have no known competing financial interests or personal relationships that could have appeared to influence the work reported in this paper.

Acknowledgements

This work was supported by the Deutsche Forschungsgemeinschaft (DFG) and the Swiss National Science Foundation (SNSF), which is gratefully acknowledged. We thank Prof. Dr. S. Grimme for calculating the CD spectra.

Appendix A. Supplementary data

Supplementary data to this article can be found online at https://doi.org/10.1016/j.ejmech.2020.112950.

References

[1] W.R. Martin, C.G. Eades, J.A. Thompson, R.E. Huppler, P.E. Gilbert, The effects of morphine- and nalorphine- like drugs in the nondependent and morphine-dependent chronic spinal dog, J. Pharmacol. Exp. Therapeut. 197 (1976) 517–532.
[2] B.D. Vaupel, Naltrexone fails to antagonize the σ-effects of PCP and SKF 10,047 in the dog, Eur. J. Pharmacol. 92 (1983) 269–274.
[3] S.B. Hellewell, W.D. Bowen, A sigma-like binding site in rat pheochromocytoma (PC12) cells: decreased affinity for (+)-benzomorphans and lower molecular weight suggest a different sigma receptor form from that of Guinea pig brain, Brain Res. 527 (1990) 244–253.
[4] S.B. Hellewell, A. Bruce, G. Feinstein, J. Orringer, W. Williams, W.D. Bowen, Rat liver and kidney contain high densities of sigma 1 and sigma 2 receptors: characterization by ligand binding and photoaffinity labeling, Eur. J. Pharmacol. 268 (1994) 9–18.
[5] M. Hanner, F.F. Moebius, A. Flandorfer, H.G. Knaus, J. Striessnig, E. Kempner, H. Glossmann, Purification, molecular cloning, and expression of the mammalian sigma1-binding site, Proc. Natl. Acad. Sci. U.S.A. 93 (1996) 8072–8077.
[6] R. Kekuda, P.D. Prasad, Y.J. Fei, F.H. Leibach, V. Ganapathy, Cloning and functional expression of the human type 1 sigma receptor (hSigmaR1), Biochem. Biophys. Res. Com. 229 (1996) 553–558.
[7] P. Seth, F.H. Leibach, V. Ganapathy, Cloning and structural analysis of the cDNA and the gene encoding the murine type 1 sigma receptor, Biochem. Biophys. Res. Commun. 241 (1997) 535–540.
[8] P. Seth, Y.-J. Fei, H.W. Li, W. Huang, F.H. Leibach, V. Ganapathy, Cloning and functional characterization of a σ receptor from rat brain, J. Neurochem. 70 (1998) 922–931.
[9] P.D. Prasad, H.W. Li, Y.-J. Fei, M.E. Ganapathy, T. Fujita, L.H. Plumley, T.L. Yang-Feng, F.H. Leibach, V. Ganapathy, Exon-intron structure, analysis of promoter region, and chromosomal localization of the human type 1 σ receptor gene, J. Neurochem. 70 (1998) 443–451.
[10] A. Alon, H.R. Schmidt, M.D. Wood, J.J. Sahn, S.F. Martin, A.C. Kruse, Identification of the gene that codes for the σ2 receptor, Proc. Natl. Acad. Sci. U.S.A. 114 (2017) 7160–7165.
[11] H.R. Schmidt, S.D. Zheng, E. Gurpinar, A. Koehl, A. Manglik, A.C. Kruse, Crystal structure of the human σ_1 receptor, Nature 532 (2016) 527–530.
[12] H.R. Schmidt, R.M. Betz, R.O. Dror, A.C. Kruse, Structural basis for sigma(1) receptor ligand recognition, Nat. Struct. Mol. Biol. 25 (10) (2018) 981–987.
[13] D.C. Mash, C.P. Zabetian, Sigma receptors Are associated with cortical Limbic areas in the primate brain, Synapse 12 (3) (1992) 195–205.
[14] N.N. Samovilova, L.V. Nagornaya, V.A. Vinogradov, (+)-[H-3]Skf 10,047 binding-sites in rat-liver, Eur. J. Pharmacol. 147 (2) (1988) 259–264.
[15] J.M. Walker, W.D. Bowen, F.O. Walker, R.R. Matsumoto, B. Decosta, K.C. Rice, Sigma-receptors - biology and function, Pharmacol. Rev. 42 (4) (1990) 355–402.
[16] C.P. Zabetian, J.K. Staley, D.D. Flynn, D.C. Mash, [H-3]-(+)-Pentazocine binding to sigma-recognition sites in human rebellum, Life Sci. 55 (20) (1994)

Pl389–Pl395.
[17] E.J. Cobos, J.M. Entrena, F.R. Nieto, C.M. Cendan, E. Del Pozo, Pharmacology and therapeutic potential of sigma(1) receptor ligands, Curr. Neuropharmacol. 6 (4) (2008) 344–366.
[18] T. Hayashi, S.Y. Tsai, T. Mori, M. Fujimoto, T.P. Su, Targeting ligand-operated chaperone sigma-1 receptors in the treatment of neuropsychiatric disorders, Expert Opin. Ther. Targets 15 (2011) 557–577.
[19] T. Hayashi, T.P. Su, sigma-1 receptor ligands – potential in the treatment of neuropsychiatric disorders, CNS Drugs 18 (5) (2004) 269–284.
[20] T. Maurice, T.P. Su, The pharmacology of sigma-1 receptors, Pharmacol. Ther. 124 (2) (2009) 195–206.
[21] T. Ishima, Y. Fujita, K. Hashimoto, Interaction of new antidepressants with sigma-1 receptor chaperones and their potentiation of neurite outgrowth in PC12 cells, Eur. J. Pharmacol. 727 (2014) 167–173.
[22] S. Collina, R. Gaggeri, A. Marra, A. Bassi, S. Negrinotti, F. Negri, D. Rossi, Sigma receptor modulators: a patent review, Exp. Op. Ther. Pat. 23 (2013) 597–613.
[23] J.L. Diaz, R. Cuberes, J. Berrocal, M. Contijoch, U. Christmann, A. Fernandez, A. Port, J. Holenz, H. Buschmann, C. Laggner, M.T. Serafini, J. Burgueno, D. Zamanillo, M. Merlos, J.M. Vela, C. Almansa, Synthesis and biological evaluation of the 1-arylpyrazole class of σ(1) receptor antagonists: identification of 4-{2-[5-methyl-1-(naphthalen-2-yl)-1H-pyrazol-3-yloxy]ethyl} morpholine (S1RA, E-52862), J. Med. Chem. 55 (2012) 8211–8224.
[24] B. Wünsch, The σ_1 receptor antagonist S1RA is a promising candidate for the treatment of neurogenic pain, J. Med. Chem. 55 (2012) 8209–8210.
[25] A. van Waarde, A.A. Rybczynska, N.K. Ramakrishnan, K. Ishiwata, P.H. Elsinga, R.A.J.O. Dierckx, Potential applications for sigma receptor ligands in cancer diagnosis and therapy, Biochim. Biophys. Acta 1848 (10) (2015) 2703–2714.
[26] F.J. Kim, C.M. Maher, sigma1 pharmacology in the context of cancer, Handb. Exp. Pharmacol. 244 (2017) 237–308.
[27] H.M. Oyer, C.M. Sanders, F.J. Kim, Small-Molecule modulators of Sigma1 and sigma2/TMEM97 in the context of cancer: foundational concepts and emerging themes, Front. Pharmacol. 10 (2019) 1141.
[28] E. Aydar, C.P. Palmer, M.B. Djamgoz, Sigma receptors and cancer: possible involvement of ion channels, Canc. Res. 64 (2004) 5029–5035.
[29] O. Soriani, S. Kourrich, The sigma-1 receptor: when adaptive regulation of cell electrical activity contributes to stimulant addiction and cancer, Front. Neurosci. 13 (2019) 1186.
[30] D. Crottes, R. Rapetti-Mauss, F. Alcaraz-Perez, M. Tichet, G. Gariano, S. Martial, H. Guizouarn, B. Pellissier, A. Loubat, A. Popa, A. Paquet, M. Presta, S. Tartare-Deckert, M.L. Cayuela, P. Martin, F. Borgese, O. Soriani, SIGMAR1 regulates membrane electrical activity in response to extracellular matrix stimulation to drive cancer cell invasiveness, Canc. Res. 76 (2016) 607–618.
[31] M. Gueguinou, D. Crottes, A. Chantome, R. Rapetti-Mauss, M. Potier-Cartereau, L. Clarysse, et al., The SigmaR1 chaperone drives breast and colorectal cancer cell migration by tuning SK3-dependent Ca(2+) homeostasis, Oncogene 36 (2017) 3640–3647.
[32] B.A. Spruce, L.A. Campbell, N. McTavish, M.A. Cooper, M.V. Appleyard, M. O'Neill, J. Howie, J. Samson, S. Watt, K. Murray, D. McLean, N.R. Leslie, S.T. Safrany, M.J. Ferguson, J.A. Peters, A.R. Prescott, G. Box, A. Hayes, B. Nutley, F. Raynaud, C.P. Downes, J.J. Lambert, A.M. Thompson, S. Eccles, Small molecule antagonists of the sigma-1 receptor cause selective release of the death program in tumor and self-reliant cells and inhibit tumor growth in vitro and in vivo, Canc. Res. 64 (2004) 4875–4886.
[33] F.J. Kim, J.M. Schrock, C.M. Spino, J.C. Marino, G.W. Pasternak, Inhibition of tumor cell growth by Sigma1 ligand mediated translational repression, Biochem. Biophys. Res. Commun. 426 (2012) 177–182.
[34] J.M. Schrock, C.M. Spino, C.G. Longen, S.M. Stabler, C. Marino, G.W. Pasternak, F.J. Kim, Sequential cytoprotective responses to sigma1 ligand-induced endoplasmic reticulum stress, Mol. Pharmacol. 84 (2013) 751–762.
[35] J.D. Thomas, C.G. Longen, H.M. Oyer, N. Chen, C.M. Maher, J.M. Salvino, B. Kania, K.N. Anderson, W.F. Ostrander, K.E. Knudsen, F.J. Kim, Sigma1 targeting to suppress aberrant androgen receptor signaling in prostate cancer, Canc. Res. 77 (2017) 2439–2452.
[36] J. Köhler, K. Bergander, J. Fabian, D. Schepmann, B. Wünsch, Enantiomerically pure 1,3-dioxanes as highly selective NMDA and σ1 receptor ligands, J. Med. Chem. 55 (2012) 8953–8957.
[37] T. Utech, J. Köhler, B. Wünsch, Synthesis of 4-(aminoalkyl) subsituted 1,3-dioxanes as potent NMDA and σ receptor antagonists, Eur. J. Med. Chem. 46 (2011) 2157–2169.
[38] T. Utech, J. Köhler, H. Buschmann, J. Holenz, J.M. Vela, B. Wünsch, Synthesis and pharmacological evaluation of a potent and selective σ_1 receptor antagonist with high antiallodynic activity, Arch. Pharm. Chem. Life Sci. 344 (2011) 415–421.
[39] R. Itooka, Y. Iguchi, N. Miyaura, Rhodium-catalyzed 1,4-addition of arylboronic acids to α,β-unsaturated carbonyl compounds: large accelerating effects of bases and ligands, J. Org. Chem. 68 (2003) 6000–6004.
[40] M.C. Viaud, P. Rollin, Zinc azide mediated Mitsunobu substitution. an expedient method for the one-pot azidation of alcohols, Synthesis (1990) 130–132.
[41] C. Xu, Z. Xiao, B. Zhuo, Y. Wang, P. Huang, Efficient and chemoselective alkylation of amines/amino acids using alcohols as alkylating reagents under mild conditions, Chem. Commun. 46 (2010) 7834–7836.
[42] C. Diedrich, S. Grimme, Systematic investigation of modern quantum chemical methods to predict electronic circular dichroism spectra, J. Phys. Chem. 107 (2003) 2524–2539.
[43] M.E. Casida, Time-dependent density functional response theory for molecules, Recent Adv. Comput. Chem. (1995) 155–192.
[44] R. Bauernschmitt, R. Ahlrichs, Treatment of electronic excitations within the adiabatic approximation of time dependent density functional theory, Chem. Phys. Lett. 256 (1996) 454–464.
[45] R. Ahlrichs, TURBOMOLE 6.0 (2009).
[46] P. Hasebein, B. Frehland, K. Lehmkuhl, R. Fröhlich, D. Schepmann, B. Wünsch, Synthesis and pharmacological evaluation of like- and unlike-configured tetrahydro-2-benzazepines with the α-substituted benzyl moiety in the 5-position, Org. Biomol. Chem. 12 (2014) 5407–5426.
[47] C. Meyer, B. Neue, D. Schepmann, S. Yanagisawa, J. Yamaguchi, E.-U. Würthwein, K. Itami, B. Wünsch, Improvement of σ1 receptor affinity by late-stage C-H-bond arylation of spirocyclic lactones, Bioorg. Med. Chem. 21 (2013) 1844–1856.
[48] K. Miyata, D. Schepmann, B. Wünsch, Synthesis and σ receptor affinity of regioisomeric spirocyclic furopyridines, Eur. J. Med. Chem. 83 (2014) 709–716.
[49] A. Banerjee, D. Schepmann, J. Köhler, E.U. Würthwein, B. Wünsch, Bioorg. Med. Chem. 18 (22) (2010) 7855–7867.
[50] M.E. Valencia, C. Herrera-Arozamena, L. de Andres, C. Perez, J.A. Morales-Garcia, A. Perez-Castillo, E. Ramos, A. Romero, D. Viña, M. Yañez, E. Laurini, S. Pricl, M.I. Rodriguez-Franco, Neurogenic and neuroprotective donepezil-flavonoid hybrids with sigma-1 affinity and inhibition of key enzymes in Alzheimer's disease, Eur. J. Med. Chem. 156 (2018) 534–553.
[51] E. Kronenberg, F. Weber, S. Brune, D. Schepmann, C. Almansa, K. Friedland, E. Laurini, S. Pricl, B. Wünsch, Synthesis and Structure–Affinity relationships of spirocyclic benzopyrans with exocyclic amino moiety, J. Med. Chem. 62 (2019) 4204–4217.
[52] I. Massova, P.A. Kollman, Combined molecular mechanical and continuum solvent approach (MM-PBSA/GBSA) to predict ligand binding, Perspect. Drug Discov. 18 (2000) 113–135.
[53] G. Grynkiewicz, M. Poenie, R.Y. Tsien, A new generation of Ca-2+ indicators with greatly improved fluorescence properties, J. Biol. Chem. 260 (6) (1985) 3440–3450.
[54] K.R. Stone, D.D. Mickey, H. Wunderli, G.H. Mickey, D.F. Paulson, Isolation of a human prostate carcinoma cell line (DU 145), Int. J. Canc. 21 (1978) 274–281.
[55] R. Vazquez, G. Civenni, A. Kokanovic, D. Shinde, J. Cantergiani, M. Marchetti, G. Zoppi, B. Ruggeri, P.C.C. Liu, G.M. Carbone, V.V. Catapano, Efficacy of novel bromodomain and extraterminal inhibitors in combination with chemotherapy for castration-resistant prostate cancer, Eur. Urol. Oncol. (2019), https://doi.org/10.1016/j.euo.2019.07.013.
[56] A.P. Hill, R.J. Young, Getting physical in drug discovery: a contemporary perspective on solubility and hydrophobicity, Drug Discov. Today 15 (2010) 648–655.
[57] S. Stegemann, F. Leveiller, D. Franchi, H. de Jong, H. Lindén, When poor solubility becomes an issue: from early stage to proof of concept, Eur. J. Pharmaceut. Sci. 31 (2007) 249–261.
[58] R.N. Waterhouse, Determination of lipophilicity and its use as a predictor of blood-brain barrier penetration of molecular imaging agents, Mol. Imag. Biol. 5 (2003) 376–389.
[59] R.A. Scherrer, S.M. Howard, Use of distribution coefficients in quantitative structure-activity relationships, J. Med. Chem. 20 (1977) 53–58.
[60] M.L. Lewis, L. Cucurull-Sanchez, Structural pairwise comparisons of HLM stability of phenyl derivatives: introduction of the Pfizer metabolism index (PMI) and metabolism-lipophilicity efficiency (MLE), J. Comput. Aided Mol. Des. 23 (2009) 97–103.
[61] D.A. Smith, K. Brown, M.G. Neale, Chromone-2-Carboxylic acids: roles of acidity and lipophilicity in drug disposition, Drug Metab. Rev. 16 (1985) 365–388.
[62] F. Galla, C. Bourgeois, K. Lehmkuhl, D. Schepmann, M. Soeberdt, T. Lotts, C. Abels, S. Ständer, B. Wünsch, Effects of polar κ receptor agonists designed for the periphery on ATP-induced Ca2+ release from keratinocytes, Med. Chem. Commun. 7 (2016) 317–326.
[63] V. Butsch, F. Börgel, F. Galla, K. Schwegmann, S. Hermann, M. Schäfers, B. Riemann, B. Wünsch, S. Wagner, Design, (Radio)Synthesis, and in vitro and in vivo evaluation of highly selective and potent matrix metalloproteinase (MMP-12) inhibitors as radiotracers for positron emission tomography, J. Med. Chem. 61 (2018) 4115–4134.
[64] G.M. Morris, R. Huey, W. Lindstrom, M.F. Sanner, R.K. Belew, D.S. Goodsell, A.J. Olson, AutoDock4 and AutoDockTools4: automated docking with selective receptor flexibility, J. Comput. Chem. 30 (2009) 2785–2791.
[65] W.L. Jorgensen, J. Chandrasekhar, J.D. Madura, R.W. Impey, M.L. Klein, Comparison of simple potential functions for simulating liquid water, J. Chem. Phys. 79 (1983) 926–935.
[66] A. Onufriev, D. Bashford, D.A. Case, Modification of the generalized born model suitable for macromolecules, J. Phys. Chem. 104 (2000) 3712–3720.
[67] Case, D.A.; Ben-Shalom, I.Y.; Brozell, S.R.; Cerutti, D.S.; Cheatham, T.E.; Cruzeiro, III, V.W.D.; Darden, T.A.; Duke, R.E.; Ghoreishi, D.; Gilson, M.K.; Gohlke, H.; Goetz, A.W.; Greene, D.; Harris, R.; Homeyer, N.; Huang, Y.; Izadi, S.;

Kovalenko, A.; Kurtzman, T.; Lee, T.S.; LeGrand, S.; Li, P.; Lin, C.; Liu, J.; Luchko, T.; Luo, R.; Mermelstein, D.J.; Merz, K.M.; Miao, Y.; Monard, G.; Nguyen, C.; Nguyen, H.; Omelyan, I.; Onufriev, A.; Pan, F.; Qi, R.; Roe, D.R.; Roitberg, A.; Sagui, C.; Schott-Verdugo, S.; Shen, J.; Simmerling, C.L.; Smith, J.; SalomonFerrer, R.; Swails, J.; Walker, R.C.; Wang, J.; Wei, H.; Wolf, R.M.; Wu, X.; Xiao, L.; York, D.M.; Kollman, P.A. AMBER 2018, University of California, San Francisco.

[68] E.F. Pettersen, T.D. Goddard, C.C. Huang, G.S. Couch, D.M. Greenblatt, E.C. Meng, T.F. Ferrin, UCSF Chimera - a visualization system for exploratory research and analysis, J. Comput. Chem. 25 (2004) 1605–1612.

[69] GraphPad prism version 6.00 for windows, GraphPad software, La jolla California USA. www.graphpad.com.